PURDUE UNIVERSITY
Purdue Research Foundation
Lafayette, Indiana

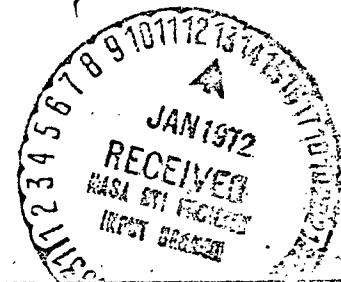Improved Fluid Dynamics Similarity,
Analysis and Verification

Final Report - Part V

ANALYTICAL AND EXPERIMENTAL STUDIES
OF THERMAL STRATIFICATION
PHENOMENA

by

E. R. F. Winter and R. J. Schoenhals

$CR-121037$

School of Mechanical Engineering
Heat Transfer Laboratory

Improved Fluid Dynamics Similarity,

Analysis and Verification

Final Report - Part V

ANALYTICAL AND EXPERIMENTAL STUDIES OF THERMAL

STRATIFICATION PHENOMENA

Submitted by

Heat Transfer Laboratory
School of Mechanical Engineering
Purdue University
Lafayette, Indiana

to

NATIONAL AERONAUTICS AND SPACE ADMINISTRATION
George C. Marshall Space Flight Center
Applied Mechanical Research Branch
Propulsion Division
Propulsion and Vehicle Engineering Laboratory
Huntsville, Alabama

Period Covered: June 29, 1965 - June 28, 1968

Principal Investigators: E. R. F. Winter and R. J. Schoenhals

Contracting Officer's Representatives: Hugh M. Campbell
William E. Dickson
Carl G. Fritz

Contract Number: NAS 8-20222
Control Number: DCN 1-5-52-01195-01 (IF) & S1 (IF)

Authors: R. I. Haug   R. J. Schonehals
          T. L. Libby   W. H. Stevenson
          R. N. Nelson   E. R. F. Winter

October 1968

INTRODUCTION

Part V of this Final Report on "Improved Fluid Dymanics Similarity, Analysis and Verification" is entitled ANALYTICAL AND EXPERIMENTAL STUDIES OF THERMAL STRATIFICATION PHENOMENA. It consists of three sections, based on a Master's thesis and two publications respectively. Because of this, each of the sections is self contained and has its own page numbering system. The titles of these sections are:

1. "Transient Stratification of Fluid in a Container Due to a Sudden Increase in Wall Temperature"

2. "An Interferometric Study of Thermal Stratification by Natural Convection in a Contained Liquid"

3. "Use of Multiple Outlets for Reducing the Stratification-Induced Propellant Supply Temperature Rise"

In the first section an analytical study of transient stratification in a rectangular container is performed using an integral method for the case in which two of the vertical walls are heated and are maintained at a constant temperature, with the remaining container walls being insulated. Experimental measurements obtained with water as the test fluid are presented. These data compare favorably with the analytical predictions for much of the transient response period. Sizeable deviations occur during the latter portion of the transient period, however, due to limitations of the analytical model in accurately describing the actual physical phenomena in this regime.

In the second section an experimental interferometric study of thermal stratification is described. In this investigation interferometer photographs were obtained. From these photographs the entire instantaneous temperature distribution can be visualized for any time during the transient stratification period. Temperature profiles obtained in this manner are compared with analytical predictions in this section, and good agreement between the two is illustrated.

In the third section a new technique is proposed for reducing the increase in the propellant supply temperature rise due to thermal stratification in the supply tank. The technique is based on proper control of the flow distribution through multiple outlets. By reducing the supply temperature rise which typically occurs during the latter portion of the engine burning period, the potential problem of cavitation in the supply pumps during this period is alleviated. Experimental measurements are given to illustrate the value of the proposed method.

SECTION 1

TRANSIENT STRATIFICATION OF FLUID IN A CONTAINER

DUE TO A SUDDEN INCREASE IN WALL TEMPERATURE[1]

---

[1]This section of Part V of the Final Report consists of a Master's thesis entitled "Transient Stratification of Fluid in a Container Due to a Sudden Increase in Wall Temperature", by Terry Lynn Libby, School of Mechanical Engineering, Purdue University, Lafayette, Indiana.

TABLE OF CONTENTS

LIST OF TABLES

LIST OF FIGURES

LIST OF SYMBOLS

Symbol	Quantity	Units
A	total wall area from which heat is transferred to the contained fluid	ft^2
A_s	cross-sectional area of the liquid	ft^2
c	specific heat	$Btu/lb_m\,°F$
g	acceleration of gravity	ft/sec^2
$\bar{h}$	average convective heat transfer coefficient	$Btu/hr\ ft^2\,°F$
H	total height of liquid in vessel	ft
k	thermal conductivity	$Btu/hr\ ft°F$
L	width of vessel	ft
$\dot{m}_{bl}$	mass flow rate in the boundary layers	lb_m/sec
P	width of heated wall	ft
q	total rate of heat transfer through the heated walls	Btu/hr
t	time	sec
$\bar{T}$	average temperature between wall and unstratified bulk liquid	°F
T_b	unstratified bulk liquid temperature	°F
T_s	surface temperature	°F
T_w	vessel inside wall temperature	°F
u	velocity of fluid within free convection boundary layer	ft/sec
u_1	velocity outside of the boundary layer of the comparable forced convection flow	ft/sec
x	coordinate measured vertically upward from vessel bottom	ft
y	coordinate measured horizontally left to right	ft

LIST OF SYMBOLS (Cont'd)

Symbol	Quantity	Units
z	coordinate measured vertically downward from liquid surface	ft

Greek Symbol	Quantity	Units
α	thermal diffusivity ($\alpha = k/c\,\rho$)	ft^2/hr
β	coefficient of expansion	$1/°F$
$\delta(x)$	boundary layer thickness	ft
Δ	stratified layer thickness	ft
θ	deviation of temperature within boundary layer from the unstratified bulk	°F
θ_w	temperature difference between wall and unstratified bulk	°F
μ	absolute viscosity	$lb_m/ft\ sec$
ν	kinematic viscosity	ft^2/sec
ρ	liquid density	lb_m/ft^3

Symbol		
C_1	combination of constant parameters (eq. 14)	$lb_m/hr\ ft^{6/5}$

$$C_1 = 0.194\ P\rho\nu(Pr)^{8/15}\left[\frac{g\beta\ (T_w - T_b)}{\nu^2}\right]^{2/5}$$

$$\left[1 + 0.494\ (Pr)^{2/3}\right]^{-2/5}$$

Gr	Grashof Number $\left(Gr = \dfrac{g\beta\ (T_w - T_b)H^3}{\nu^2}\right)$	None
Pr	Prandtl Number ($Pr = c\,\mu/k$)	None

LIST OF SYMBOLS (Cont'd)

Symbol	Quantity	Units
Gr*	modified Grashof Number used in Reference 4	None

$$\left(Gr^* = \frac{g\beta\dot{q}H^4}{k\,\nu^2} \right)$$

ϕ	dimensionless time used in Reference 4	None

$$(\phi = \nu t/H^2)$$

$\dot{q}$	heated wall heat flux used in Reference 4	Btu/hr ft^2
R	radius of vessel used in Reference 4	ft
I	energy integral used in Reference 4	None

$$\left(I = \int_0^1 \frac{T-T_s}{T_s-T_b} \, d\,(z/\Delta) \right)$$

ABSTRACT

This investigation was undertaken to determine the stratification behavior of a contained fluid subjected to transient free convection heat transfer. The motivation for this study was provided by the fact that stratification processes are encountered in cryogenic fluids used in liquid propellant rockets. For convenience, water was used as the test liquid in conducting the experiments. A rectangular vessel was employed with heat transfer from two opposite walls of the vessel to the fluid. The wall temperature was increased suddenly to initiate the process and was then maintained constant throughout the transient stratification period. Thermocouples were positioned on a post at the center of the vessel. They were adjusted so that temperatures could be measured at the fluid surface and at specific depths beneath the surface.

A major goal of this work was the attainment of analytical and experimental results for the surface temperature and for the stratified layer thickness. The predicted values of the surface temperature and the stratified layer thickness were found to agree reasonably well with the experimental measurements. The experiments also provided information on the transient centerline temperature distribution and the transient flow distribution.

INTRODUCTION

When a fluid contained in a vessel is subjected to external heating, a process known as stratification takes place. In this process the warmer fluid tends to rise to the top of the vessel due to its buoyancy, and this causes the fluid to be formed into horizontal layers having different temperatures. For this particular study the heat transfer occurred through two opposite walls of a rectangular vessel, as shown in Figure 1.

The heat transfer through the container walls results in the creation of a free convection boundary layer along each wall. As the fluid in the boundary layer becomes heated it rises and is simultaneously replaced by the colder bulk fluid near the bottom of the vessel. When the fluid rising along the wall reaches the surface, it leaves the boundary layer and flows across the surface toward the geometric center of the vessel. The flows from both boundary layers meet at the center of the symmetrical vessel. Here they form a plume which moves downward into the bulk liquid region. This downward motion of the plume is arrested rapidly and is reversed by buoyancy effects. The warmer fluid in the plume then moves upward and outward simultaneously, forming a nearly uniform layer of fluid called the stratified layer. As the process continues the surface temperature increases with an ever decreasing rate and approaches a maximum value. Simultaneously, the stratified layer thickness approaches the total fluid depth with

Legend:

q - Heat Transfer through Walls

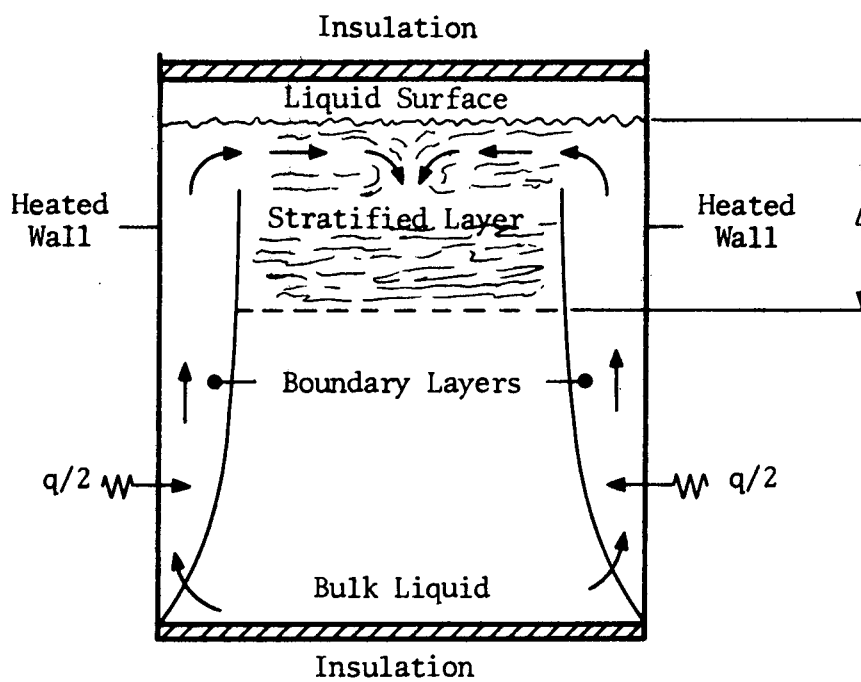Δ - Stratified Layer Thickness

FIGURE 1. CROSS SECTION OF A STRATIFYING FLUID
CONTAINED IN A VESSEL WITH HEATED WALLS

a decreasing rate. A more complete explanation of the stratification process is given in the following section of this report. For purposes of the present discussion the brief description given above will suffice.

The stratification of cryogenic fluids is very important in situations where these fluids are used as rocket propellants. In these cases the bulk liquid temperature is very low, and large temperature differences typically exist between the bulk liquid and the environment. This causes large heat transfer rates to the fluid which can cause a sizeable fraction of the fluid to become heated and stratified. When this heated fluid is pumped rapidly to the engine during flight, its high temperature can cause cavitation to occur. A condition such as this in the pumps can choke off the propellant flow to the engines, and thus lead to premature engine burnout.

The significance of stratification is not limited to the space industry. The stratification of a lake is beneficially put to use by knowledgeable fishermen. It is a verified fact that different fish desire different water temperatures. These temperatures are created by the stratification of the lake's water, and a knowledge of this phenomenon is a helpful aid to the fisherman.

In the present investigation the fluid was contained in a rectangular vessel which permitted heat transfer through only two parallel walls (Figure 1). The remaining walls were insulated. The stratification process was experimentally studied, and the measurements were compared with the corresponding predictions obtained by analysis. For convenience, water was used as the test liquid. A constant wall temperature was imposed at the heated surfaces. Experimentally, this was

obtained by suddenly flowing hot water at a preset temperature over the outside of the two walls of the vessel.
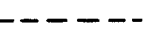
An approximate integral method was used in the analysis to obtain equations which govern the stratification process. The use of this method implies that solutions of the resulting equations are not exact in their description of the stratification process. The analytical results are therefore not quantitatively precise, but they are qualitatively correct. For this reason they serve very well the purpose of providing good approximate results of the process.

In the following section the stratification process is described in further detail. Then a review is given of previous articles and reports describing investigations which have been conducted on the phenomena of stratification in order to provide sufficient background material. The specific problem investigated in this study is treated in the remainder of this presentation.

DETAILED DESCRIPTION OF THE STRATIFICATION PROCESS

In this section a detailed physical description of the stratification process is given. The various features which are discussed here are well known from previous investigations. Some of these previous studies are reviewed in the following section of this report.

As stated in the Introduction, the heat transfer through the two walls creates a free convection boundary layer along each wall adjacent to the body of stationary fluid. The fluid in these boundary layers becomes heated and consequently decreases in density. This decrease in density, together with the gravitational field, creates an upward buoyancy force and flow within the boundary layers. The fluid moving up and finally out of the boundary layers is supplemented by fluid moving into the boundary layers in the bottom portion of the vessel. This latter fluid which continuously replenishes the boundary layers comes from the bulk fluid. The heated fluid continues up the entire height of the boundary layer to the surface. This hot fluid then continues across the surface in a direction normal to the heated walls and inward toward the center of the vessel. The flows from the two boundary layers meet just below the liquid surface at the center of the vessel. At this point they form a plume which moves downward toward the bulk fluid. The initial phase of the stratification process is depicted in Figure 2a. The process continues as the downward motion of the plume is arrested and is finally reversed due to buoyancy effects.
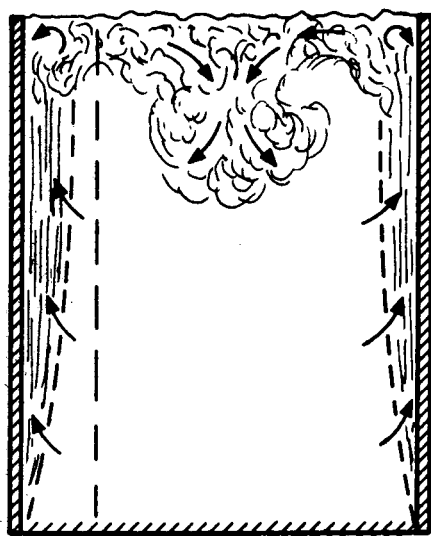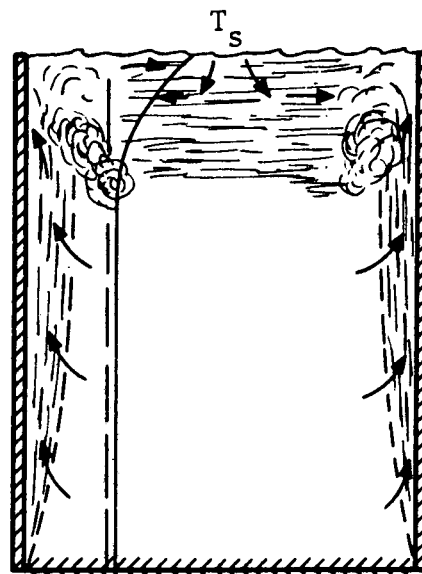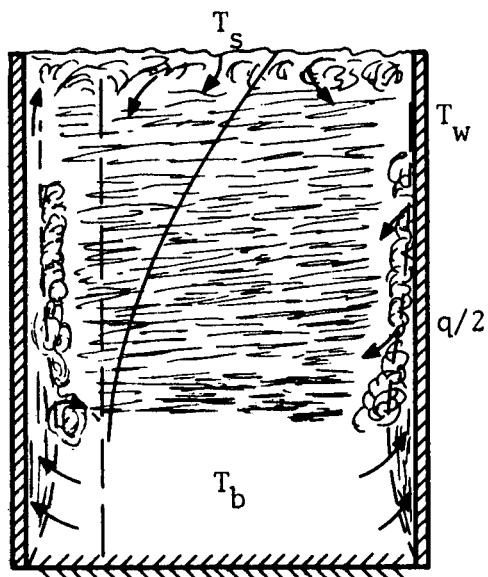
FIGURE 2. STAGES OF THE STRATIFICATION PROCESS

The warmer fluid within the plume then moves upward and outward simultaneously, forming a layer of fluid of nearly uniform thickness called the stratified layer. At the same time, a reverse shear layer is formed as shown by the darkened area impinging on the boundary layer (Figure 2b). The vorticity within this layer tends to induce downward motion in the rising fluid as well as motion across the fluid bulk under the stratified layer. As the process proceeds, the reverse shear layer becomes less pronounced due to its gradual suppression by the growing stratified layer. Likewise, the part of the boundary layer congruent with the stratified layer becomes very thin, as shown in Figure 2c. In this manner the entire fluid bulk eventually becomes stratified. As long as the boundary layers are maintained, the process continues until the entire fluid bulk reaches a uniform temperature equal to the temperature of the container walls.

As a final note, the bulk fluid receives some heat by conduction from the stratified layer. An order of magnitude analysis shows that this effect is very small for time periods which are typical of the stratification process.

PREVIOUS INVESTIGATIONS OF STRATIFICATION PHENOMENA

The stratification process has been studied by a number of investigators. An experimental investigation of the stratification of a cryogenic fluid contained in a vessel was carried out by Scott et al. (Reference 1). It was found that the presence of a good heat conducting rod placed vertically within the liquid provided a path for heat conduction and eliminated the stratification tendencies of liquid helium contained in a nonventing Dewar vessel.

Anderson et al. (Reference 2) have given an approximate mathematical method for the analysis of the stratification of a contained fluid for the situation in which the vessel walls are heated by radiation. Barakat (Reference 3), on the other hand, presents an exact mathematical method for the description of the flow patterns during the stratification process.

A literature survey, carried out as a portion of the present study, revealed that most of the investigations conducted on stratification phenomena employed very specific conditions. Primarily, these conditions either involved the method by which the vessel walls were heated or were concerned with the geometric shape of the vessel itself. For instance, Tellep and Harper (Reference 4) employed a cylindrical container for analyzing the stratification of a liquid (water) receiving a constant heat flux from the surroundings. Ruder (Reference 5) pressurized a contained fluid and discovered that the temperature profile

in the stratified layer had a shape similar to a Gaussian probability distribution function.

Eckert and Jackson (Reference 6) do not deal specifically with stratification, but present an analytical study of a turbulent free convection boundary layer on a flat plate. The equations derived in their work provided the boundary layer temperature and velocity profile expressions used in the present study.

Schwind and Vleit (Reference 7) present a very descriptive discussion of the entire stratification process including the phenomenon of the reverse shear layer. Briefly, the reverse shear layer forms in a region between the boundary layer and the stratified section of the fluid core. This phenomenon occurs due to very complicated fluid particle motions.

Unlike the side wall heating arrangement in the present investigation, Duke (Reference 8) heated a vessel at the bottom. This vessel was cylindrical in shape and had a conical bottom. Despite the significant difference in design between this vessel and the one used for the present study, the temperature profiles in the respective stratified layers were found to be similar in shape.

Bailey, et al. (Reference 9) studied the phenomenon of stratification of a cryogenic propellant. The analytical work was based on the approximate integral method which was also used in the present study. The container was cylindrical in shape. The equations were essentially identical to those used by Tellep and Harper (Reference 4). In this study, however, the analytical results were compared with actual data obtained from the propellant tanks of the Titan and Vanguard missiles.

Churchill (Reference 10) was not concerned with stratification, rather the significance here lies in the mathematical method used in the present study. The primary discussion was concerned with the attempts which have been made to predict natural convection phenomena. The study compares the classical methods of analysis, such as the approximate integral method employed in the present study, with the various new numerical techniques.

A great deal of effort has been devoted to the phenomenon of stratification. Many of these previous studies were conducted with cryogenic fluids. These reports are listed under Additional References to provide a broader background for the present study.

DIMENSIONAL ANALYSIS

In previous sections it has been explained that free convection heat transfer is the primary mechanism for energy transport in the stratification process. Free convection heat transfer has been thoroughly studied by many investigators. The results of these investigations disclose the parameters involved in the free convection heat transfer process, and consequently, the parameters imposed on the stratification process. In view of the knowledge of the free convection parameters, the stratified layer thickness (Δ) can be appropriately represented by

$$\Delta = f \left[\rho, \ c, \ k, \ t, \ g, \ \beta, \ \mu, \ (T_w - T_b), \ H, \ P, \ A_s \right] \tag{1}$$

The system is illustrated in Figure 3.

The stratified layer thickness (Δ) is dependent on:

(1) the elapsed time (t)

(2) the physical properties of the fluid such as density (ρ); viscosity (μ); conductivity (k); specific heat (c); and the thermal coefficient of expansion (β)

(3) the gravitational field (g)

(4) the heat transfer rate which is directly related to the temperature difference $(T_w - T_b)$

(5) the dimensions of the vessel, such as the height (H); the heated perimeter (P); and the area of fluid cross-section (A_s).

Equation (1) above expresses the stratified layer thickness (Δ) as a

TOP VIEW

Adiabatic

Adiabatic

FRONT VIEW

Adiabatic

Adiabatic
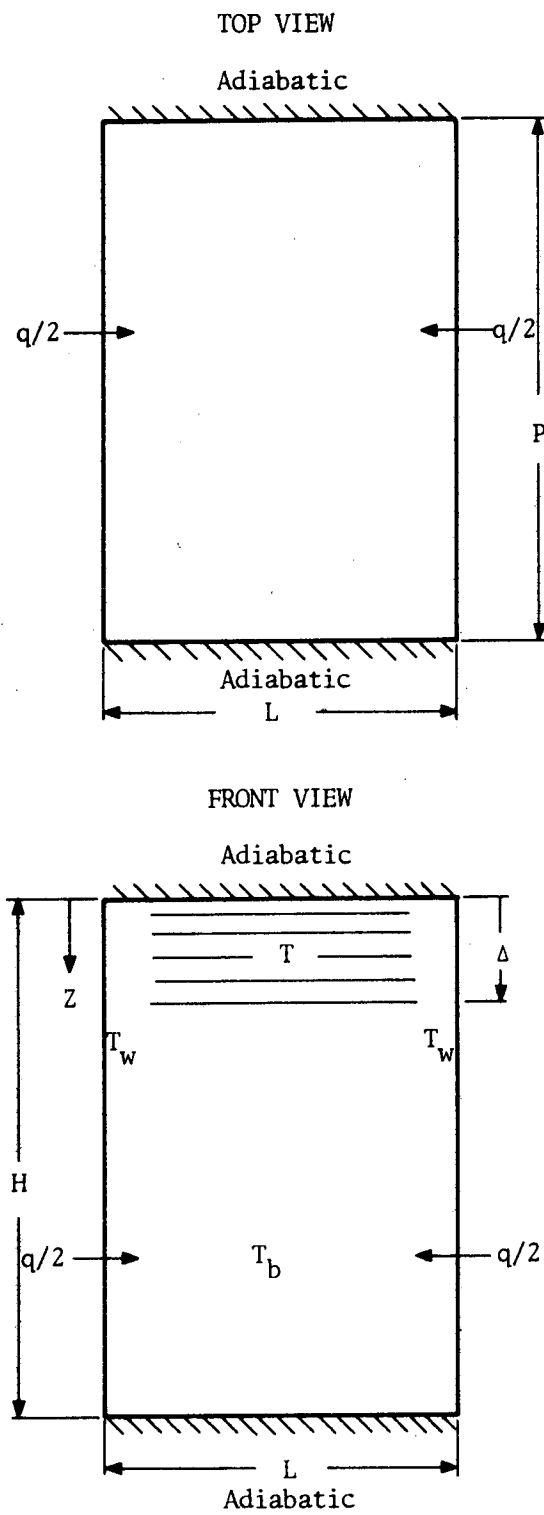
FIGURE 3.   STRATIFICATION PARAMETERS

function of these parameters. Table 1 below lists these parameters with their corresponding fundamental dimensions of mass (M); time (t); length (L); and temperature (T).

Table 1. Fundamental Dimensions

Symbol	Parameter	Dimensions
Δ	stratified layer thickness	L
k	thermal conductivity	$MLt^{-3}T^{-1}$
ρ	density	ML^{-3}
c	specific heat	$L^2t^{-2}T^{-1}$
t	time	t
g	gravitational field	Lt^{-2}
β	coefficient of expansion	T^{-1}
(T_w-T_b)	wall to bulk liquid temperature difference	T
H	height of liquid in the vessel	L
μ	dynamic viscosity	$ML^{-1}t^{-1}$
P	width of heated wall	L
A_s	cross-sectional area of the liquid	L^2

The dimensions associated with equation (1) can be represented by

$$L = \left[MLt^{-3}T^{-1}\right]^a \left[ML^{-3}\right]^b \left[L^2t^{-2}T^{-1}\right]^c \left[t\right]^d \left[Lt^{-2}\right]^e$$
$$\left[T^{-1}\right]^f \left[T\right]^g \left[L\right]^h \left[ML^{-1}t^{-1}\right]^i \left[L\right]^j \left[L^2\right]^k \qquad (2)$$

Since L alone exists on the left-hand side of equation (2), the sum of the exponents of the three remaining dimensions on the right-hand side must be zero. Accordingly, the sum of the exponents of L on the right-hand side of the equation must be one (1). Listed below in Table 2 are

the four (4) dimensions and their corresponding exponents summed to the appropriate values as indicated above. The ensuing operations follow the method of Buckingham's Π-Theorem.

Table 2. Exponent Equations

Dimension	Exponents		
M	$a + b$	$+ i$	$= 0$
L	$a -3b +2c + e$	$+ h - i + j +2k$	$= 1$
t	$-3a -2c + d -2e$	$- i$	$= 0$
T	$- a - c - f + g$		$= 0$

The four (4) equations contain eleven (11) unknowns; thus, four (4) of the unknown exponents can be solved in terms of the other seven (7). The exponents chosen are a, c, g, and h, respectively. These exponents are found in terms of the remaining exponents using the equations as given in Table 2. Equation (1) can now be written as

$$\Delta = (k)^{-b-i} (\rho)^b (c)^{3/2b+i-e+1/2d} (t)^d (g)^e (\beta)^f$$

$$(T_w-T_b)^{f+1/2b-e+1/2d} (H)^{1+b-d+e-j-2k} (\mu)^i (P)^j (A_s)^k \qquad (3)$$

Rearrangement of this equation leads to

$$\frac{\Delta}{H} = \left[k^{-1}\rho c^{3/2} (T_w-T_b)^{1/2}H \right]^b \left[c^{1/2}t (T_w-T_b)^{1/2}H^{-1} \right]^d$$

$$\left[c^{-1}g (T_w-T_b)^{-1}H \right]^e \left[\beta (T_w-T_b) \right]^f \left[c \mu k^{-1} \right]^i$$

$$\left[PH^{-1} \right]^j \left[A_sH^{-2} \right]^k \qquad (4)$$

Equation (4) indicates that

$$\frac{\Delta}{H} = F\left[\frac{\rho c^{3/2}(T_w-T_b)^{1/2}H}{k}, \frac{c^{1/2}t(T_w-T_b)^{1/2}}{H}, \frac{gH}{c(T_w-T_b)},\right.$$
$$\left.\beta(T_w-T_b), \frac{\mu c}{k}, \frac{P}{H}, \frac{A_s}{H^2}\right] \qquad (5)$$

Some of the seven (7) Π-factors which appear on the right-hand side of equation (5) can be rearranged to give more familiar dimensionless groups. By carrying out the necessary manipulations, the expression for $\frac{\Delta}{H}$ can be rewritten as

$$\frac{\Delta}{H} = G\left[\frac{t}{\sqrt{H/g}}, \frac{\mu c}{k}, \frac{\rho^2 g\beta(T_w-T_b)H^3}{\mu^2}, \frac{gH}{c(T_w-T_b)},\right.$$
$$\left.\frac{\rho c^{3/2}(T_w-T_b)^{1/2}H}{k}, \frac{P}{H}, \frac{A_s}{H^2}\right] \qquad (6)$$

The dimensionless groups in expression (6) are given descriptive names below.

(1) $\frac{\Delta}{H}$, dimensionless stratified layer thickness

(2) $\frac{P}{H}$, geometry of container

(3) $\frac{A_s}{H^2}$, geometry of container

(4) $\frac{t}{\sqrt{H/g}}$, dimensionless time

(5) $\frac{g\rho^2\beta(T_w-T_b)H^3}{\mu^2}$, Grashof Number

(6) $\frac{\mu c}{k}$, Prandtl Number

(7) $\dfrac{gH}{c(T_w-T_b)}$, ratio of potential energy to thermal energy

(8) $\dfrac{\rho c^{3/2}(T_w-T_b)^{1/2}H}{k}$, dimensionless diffusion of thermal energy

The above results show that no less than eight (8) dimensionless groups are pertinent to the stratification process. This information serves as a guide for the analysis to follow.

ANALYSIS

There are two major objectives of the analysis presented in this section. The first is to obtain a relation between the stratified layer thickness (Δ) and elapsed time (t). The second is to determine the temperature distribution in the stratified layer and, simultaneously, to obtain the liquid surface temperature (T_s) variation with time. The fluid is considered to have an initially uniform temperature (T_b). The various parameters used in the analysis are shown in Figure 4.

The first portion of the analysis involves the derivation of an expression for the growth of the stratified layer based on the mass flow rate ($\dot{m}_{bl}$) in the boundary layers. From this foundation and from a consideration of the internal energy of the stratified layer, it is possible to determine the approximate temperature distribution and the rate of increase of the liquid surface temperature (T_s).

Certain assumptions are made for the purpose of promoting a straight forward step-by-step analysis resulting in the determination of these expressions. This procedure leads to analytical predictions which are compared with experimental measurements. The assumptions made in the analysis are the following:

1. The heat transfer rate from the heated walls to the contained fluid remains constant throughout the transient stratification period, and equal to the actual rate existing just after the process is initiated. In reality, the heat transfer rate

Legend:

q - Heat Transfer through Walls

$\delta(x)$ - Boundary Layer Thickness

Δ - Stratified Layer Thickness

T_w - Inside Wall Temperature

T_s - Surface Temperature

T_b - Bulk Temperature

$\dot{m}_{bl}$ - Mass Flow Rate in Boundary Layers
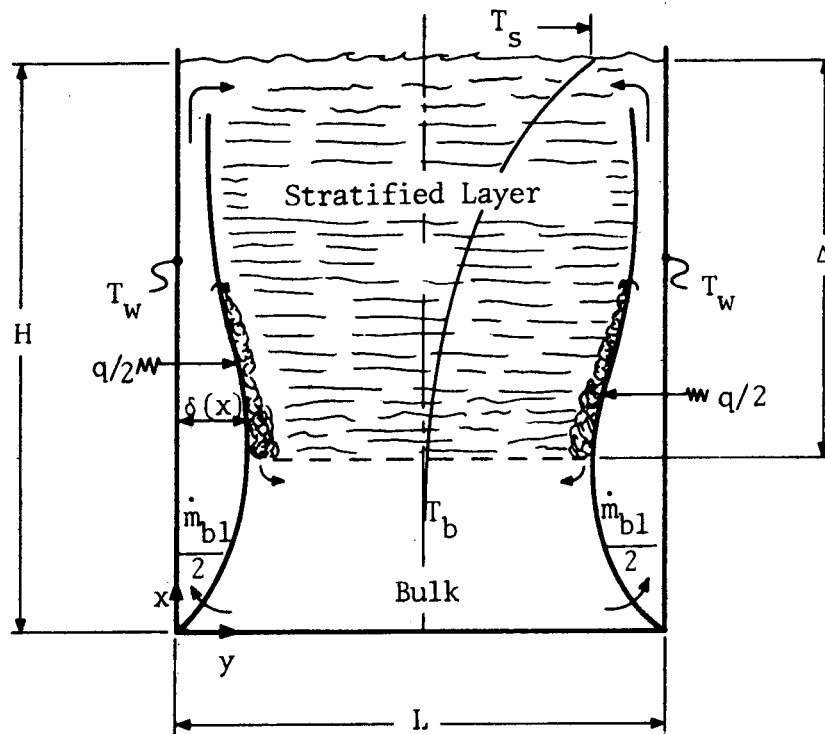
FIGURE 4. DESCRIPTION OF PARAMETERS USED IN ANALYSIS

decreases with time to some extent, since the heat flux from the portion of the heated walls adjacent to the stratified layer is attenuated by the increased fluid temperature levels in the upper portion of the tank. Consequently, the rate of increase of the surface temperature (T_s) as determined by this analysis is somewhat higher than that which actually occurs.

2. There is no heat transfer from the boundary layers or from the stratified layer to the bulk fluid below the stratified layer; therefore, the bulk temperature (T_b) remains constant throughout the stratification process.

3. The convection heat transfer coefficient ($\bar{h}$) is calculated according to (Reference 11):

$$\bar{h} = 0.021 \frac{k_f}{H} (GrPr)^{2/5} \qquad (1)$$

for a turbulent boundary layer ($GrPr > 10^{10}$). However, when the GrPr product is in the neighborhood of $10^8 - 10^{10}$, the heat transfer coefficient is determined by using the following correlation (Reference 11):

$$\bar{h} = 0.12 \frac{k_f}{H} (GrPr)^{1/3} \qquad (2)$$

The corresponding expression for a laminar boundary layer is not presented here, since it is assumed that the boundary layers existing in typical stratification processes are either in the transitional or fully turbulent range. (This contention is illustrated in a subsequent section of this report which deals with the experimental results.)

The definitions of the symbols appearing in the preceding expressions are given below:

$\bar{h}$ = average convection heat transfer coefficient in $\dfrac{Btu}{hr\text{-}ft^2\,°F}$

k_f = thermal conductivity of the fluid in $\dfrac{Btu}{hr\text{-}ft\,°F}$

H = height of the contained fluid in ft

T_w = inside wall temperature in °F

T_b = bulk fluid temperature in °F

β = coefficient of thermal expansion in $°F^{-1}$

c = specific heat in $\dfrac{Btu}{Lbm\,°F}$

ν = kinematic viscosity in $\dfrac{ft^2}{sec}$.

4. All fluid properties are assumed to be constant.

5. The temperature profile in the stratified layer is assumed to be well approximated by a parabola (see Figure 4).

6. The boundary layers are very thin such that the boundary layer response can be assumed as instantaneous compared with the rest of the system. Thus, it is assumed that steady state velocity and temperature boundary layer profiles apply. Hence, the thermal inertia of the boundary layers is neglected.

The statements 1 through 6 above complete the list of assumptions and conditions incorporated into the analysis.

The thermal conditions discussed under assumption 2 require some further explanation. The heated region at the top of the container in reality extends slightly below the stratified layer as a result of heat conduction between the stratified layer and the colder bulk fluid below it. However, in order to simplify the analytical

description of the stratification process, it is assumed that the heat transfer occurring between the stratified layer and the bulk fluid is negligible. This implies that the thickness of the heated layer at the top is essentially equal to that of the stratified layer. This is a reasonable assumption since transient heat conduction effects can be shown to be small for time periods which are typical of the stratification process, as mentioned previously.

The goal of the present analysis is to formulate a simple mathematical model of the stratification phenomenon by considering only the dominant physical processes. Thus, the resulting analytical predictions are necessarily approximate and must be regarded as qualitative, primarily due to the fact that the extension of the heated region below the stratified layer is not treated. Nevertheless, the analysis does yield approximate solutions which provide the proper trends and orders of magnitude for the important parameters of interest. This fact was established on the basis of experimental measurements to be presented later in this report. These measurements also indicate that the growth of this heated region does not appreciably influence the rate of growth of the stratified layer until far into the transient period when the heated portion of the bulk liquid extends nearly to the bottom of the container.

Refer now to Figure 4 and consider the boundary layer to be turbulent. Eckert and Jackson (Reference 6) give approximations to the velocity (u) and temperature (θ) profiles for a turbulent boundary layer as

$$u = u_1 \ (y/\delta)^{1/7} \ (1-y/\delta)^4 \tag{3}$$

$$\theta = \theta_w \left[1 - (y/\delta)^{1/7} \right] \tag{4}$$

where

u_1 = velocity outside of the boundary layer of the comparable forced convection flow

θ = deviation of temperature within boundary layer from the bulk fluid temperature = $(T-T_b)$

θ_w = temperature difference between the wall and the bulk fluid = (T_w-T_b)

u = velocity of the fluid within the free convection boundary layer

The expression for u_1 is also obtained from Reference 6 as

$$u_1(x) = 1.185 \ (\nu/x) \ Gr^{1/2} \left[1 + 0.494 \ (Pr)^{2/3}\right]^{-1/2} \qquad (5)$$

where

x = coordinate measured upward from the container bottom

$\delta(x)$ = boundary layer thickness

Also from Reference 6, $\delta(x)$ is given by

$$\delta(x) = 0.565x \ (Gr)^{-1/10} \ (Pr)^{-8/15} \left[1 + 0.494 \ (Pr)^{2/3}\right]^{1/10} \qquad (6)$$

The mass flow rate in the two boundary layers, at a distance x from the vessel bottom, is obtained by integrating the velocity (u) over the boundary layer thickness. Thus,

$$\dot{m}_{b1}(x) = 2P \int_0^{\delta(x)} \rho u \, dy \qquad (7)$$

where P is the width of each heated wall. Since the value of the fluid density (ρ) is taken to be constant, the expression for the mass flow rate becomes

$$\dot{m}_{b1}(x) = 2P\rho \int_0^{\delta(x)} u \, dy \qquad (8)$$

The relation for the velocity as a function of distance from the wall, equation (3), is substituted for u in equation (8). The result is

$$\dot{m}_{b1}(x) = 2P\rho \int_0^{\delta(x)} u_1(x) \, [y/\delta(x)]^{1/7} \, [1 - y/\delta(x)]^4 \, dy \qquad (9)$$

The variable of integration (y) is now changed to $y/\delta(x)$ by rewriting equation (9) as

$$\dot{m}_{b1}(x) = 2P\rho\delta(x) \, u_1(x) \int_0^1 [y/\delta(x)]^{1/7} \, [1 - y/\delta(x)]^4 \, d[y/\delta(x)] \qquad (10)$$

Integration of this expression yields

$$\dot{m}_{b1}(x) = 2P\rho \, [0.145 \, \delta(x) \, u_1(x)] \qquad (11)$$

The previously given expressions for $u_1(x)$ and $\delta(x)$, equations (5) and (6), are now substituted into the above equation, and the final expression for the mass flow rate is obtained as

$$\dot{m}_{b1}(x) = 2P\rho \left\{ 0.097 \; \nu \; (Gr)^{2/5} \; (Pr)^{8/15} \left[1 + .494 \; (Pr)^{2/3} \right]^{-2/5} \right\} \qquad (12)$$

Since the growth of the stratified layer comprises the first objective of this analysis, the mass flow rate $(\dot{m}_{b1})$ is evaluated at its location of entrance to the stratified layer. Specifically, the mass flow rate $(\dot{m}_{b1})$ is calculated at the lower boundary of the stratified layer where $x = H - \Delta$. Thus, equation (12) becomes

$$\left[\dot{m}_{bl}(x)\right]_{x = H - \Delta} = 2P\rho \left\{ 0.097\nu \left[\frac{g\beta (T_w - T_b)(H-\Delta)^3}{\nu^2}\right]^{2/5} (Pr)^{8/15} \left[1 + .494 (Pr)^{2/3}\right]^{-2/5} \right\} \tag{13}$$

which gives the mass flow rate across the lower boundary of the stratified layer. Notice that equation (13) can be written in simplified form as

$$\left[\dot{m}_{bl}(x)\right]_{x = H - \Delta} = \text{Constant } (H-\Delta)^{6/5} = C_1 (H-\Delta)^{6/5} \tag{14}$$

where $C_1 = 0.194 \, P\rho \, \nu \left[\dfrac{g\beta(T_w - T_b)}{\nu^2}\right]^{2/5} (Pr)^{8/15} \left[1 + .494(Pr)^{2/3}\right]^{-2/5}$

$$\frac{\text{lbm}}{\text{hr-ft}^{6/5}}$$

Another expression containing the boundary layer mass flow rate $(\dot{m}_{bl})$ can be developed by applying the law of conservation of mass to the stratified layer. This expression is

$$\left[\dot{m}_{bl}(x)\right]_{x = H - \Delta} = \frac{d}{dt} (\rho A_s \Delta) = \rho A_s \frac{d\Delta}{dt} \tag{15}$$

Combining equations (14) and (15) results in

$$\rho A_s \frac{d\Delta}{dt} = C_1 (H-\Delta)^{6/5} \tag{16}$$

Equation (16) can be integrated to determine the relation for Δ as a function of time (t). Thus, separating variables leads to

$$\frac{d\Delta}{(H-\Delta)^{6/5}} = \frac{C_1 dt}{\rho A_s} \tag{17}$$

Integration produces

$$5(H-\Delta)^{-1/5} = \frac{C_1 t}{\rho A_s} + K_1 \tag{18}$$

where K_1 is a constant of integration. K_1 is determined by applying the boundary condition that $\Delta = 0$ at $t = 0$. From equation (18) the result is

$$K_1 = 5H^{-1/5} \qquad (19)$$

Consequently, equation (18) can be rewritten as

$$5(H-\Delta)^{-1/5} = \frac{C_1 t}{\rho A_s} + 5H^{-1/5} \qquad (20)$$

The stratified layer thickness (Δ) can be obtained as a function of time (t) through the rearrangement of this expression. Thus,

$$\frac{\Delta}{H} = 1 - \left[1 + \frac{C_1 H^{1/5} t}{5\rho A_s} \right]^{-5} \qquad (21)$$

The constant factor C_1 can now be replaced by its corresponding parametric expression as obtained from equation (13). This operation yields

$$\frac{\Delta}{H} = 1 - \left\{ 1 + .0388\, \nu \left(\frac{P}{A_s} \right) (Pr)^{8/15} \left[\frac{g\beta\, (T_w - T_b)}{\nu^2} \right]^{2/5} \right.$$
$$\left. \left[1 + .494\, (Pr)^{2/3} \right]^{-2/5} H^{1/5} t \right\}^{-5} \qquad (22)$$

Equations (21) and (22) express the growth of the stratified layer thickness (Δ) as a function of time (t). It remains at this point in the analysis to determine the variation of the surface temperature (T_s) as a function of time (t). The surface temperature (T_s) can be inserted into the expression which equates the rate of convective heat transfer from

the heated walls to the change in internal energy occurring within the stratified layer. This expression is

$$q = \rho A_s c \frac{d}{dt} \int_0^\Delta (T-T_b)dz \qquad (23)$$

where

q = heat transfer rate in Btu/hr

A_s = cross-sectional area of fluid in ft^2

t = elapsed time in sec

c = specific heat in $\frac{Btu}{lbm \, ^\circ F}$

Δ = stratified layer thickness in ft

z = coordinate measured from the liquid surface downward

Equation (23) is now rewritten as

$$q = \rho A_s c \frac{d}{dt} \left\{ (T_s - T_b) \, \Delta \int_0^1 \left[\frac{T - T_b}{T_s - T_b} \right] d \left(\frac{z}{\Delta} \right) \right\} \qquad (24)$$

In order to carry out the integration of equation (24), the quantity

$$\left(\frac{T - T_b}{T_s - T_b} \right)$$

must be known as a function of z/Δ. At this point assumption 5 is employed. Accordingly, the approximation for the dimensionless temperature profile in the stratified layer is written as

$$\frac{T - T_b}{T_s - T_b} = [1 - z/\Delta]^2 \qquad (25)$$

This approximation has been used previously by Tellep and Harper (Reference 4), who offered considerable evidence of its validity for

their investigation. The justification for using this procedure in the present development is based on the experimental temperature measurements by Tellep and Harper as well as those of the present study. Tellep and Harper found that use of this expression for the temperature profile gave rise to a predicted rate of growth for the stratified layer which compared very well with their experimental results. However, there was a sizeable deviation between the analytical prediction and the measured data when the stratified layer approached the container bottom. Tellep and Harper's results are compared with those of this study in a following section of this report. The insertion of equation (25) into equation (24), followed by evaluation of the integral, produces

$$q = 1/3 \; \rho A_s c \; \frac{d}{dt} \; [(T_s - T_b) \; \Delta] \qquad (26)$$

An exact integration of equation (26) is not achievable at this stage of the analysis, since the time dependency of the left-hand side (q) is not known. Here it is assumed that the heat transfer through the heated walls remains constant throughout the entire transient period, and equal to the actual rate occurring immediately after initiation of the process (assumption 1). Thus,

$$q = \bar{h} A \; (T_w - T_b) = \text{Constant} \qquad (27)$$

where

q = heat transfer rate in Btu/hr

$\bar{h}$ = average convection heat transfer coefficient at the start of the process in $\dfrac{Btu}{hr\text{-}ft^2 \; °F}$

A = total wall area from which heat is transferred to the contained fluid, 2PH in ft^2

P = width of the wall in ft

H = total depth of the fluid in ft

As mentioned previously in the discussion of assumption 1, the actual heat transfer rate can be expected to decrease with time to somewhat lower values as stratification proceeds. Therefore, the predicted variation of surface temperature (T_s) with time (t) can be expected to be above that which occurs in reality. Insertion of equation (27) into equation (26) yields

$$q = \bar{h}A \ (T_w - T_b) = \text{Constant} = 1/3 \ \rho A_s c \ \frac{d}{dt} \ [(T_s - T_b) \ \Delta] \qquad (28)$$

or

$$\frac{d}{dt} \ [(T_s - T_b) \ \Delta] = \frac{3q}{\rho A_s c} = K \ \text{(constant)} \qquad (29)$$

Integration of equation (29) yields

$$(T_s - T_b) \ \Delta = Kt + E \qquad (30)$$

where E is a constant of integration. Consideration of the two initial conditions, $\Delta = 0$ and $(T_s - T_b) = 0$ at $t = 0$, leads to the conclusion that the constant E must equal zero also. Equation (30) is now solved for the temperature difference with Δ replaced by its equivalent expression given in equation (21). Thus,

$$(T_s - T_b) = \frac{Kt}{\Delta} = \frac{Kt}{H \left\{ 1 - \left[1 + \dfrac{C_1 H^{1/5} t}{5 \rho A_s} \right]^{-5} \right\}} \qquad (31)$$

Substituting the expression for K from equation (29) yields

$$(T_s - T_b) = \frac{3hA\,(T_w - T_b)\,t}{\rho A_s Hc \left\{ 1 - \left[1 + \frac{C_1 H^{1/5} t}{5 \rho A_s} \right]^{-5} \right\}} \qquad (32)$$

The combination of parameters, $\rho A_s H$, in the denominator of equation (32) is actually the total mass of liquid in the container. Equation (32) can be nondimensionalized by dividing through by the temperature difference $(T_w - T_b)$ which yields

$$\frac{T_s - T_b}{T_w - T_b} = \frac{6hPt}{\rho A_s c \left\{ 1 - \left[1 + \frac{C_1 H^{1/5} t}{5 \rho A_s} \right]^{-5} \right\}} \qquad (33)$$

where the heat transfer area, A, has been replaced by 2PH. A final expression for the temperature difference is obtained by substituting the full expression for the constant C_1 from equation (13). Thus,

$$\frac{T_s - T_b}{T_w - T_b} =$$

$$\frac{\left(\frac{6\bar{h}}{\rho Lc}\right) t}{\left\{ 1 - \left[1 + .0388 \left(\frac{\nu}{L}\right) \left[\frac{g\beta(T_w - T_b)}{\nu^2}\right]^{2/5} (Pr)^{8/15} \left[1 + .494(Pr)^{2/3}\right]^{-2/5} H^{1/5} t \right]^{-5} \right\}} \qquad (34)$$

where A_s, the liquid cross-sectional area, has been replaced by the product of P and L which are the heated and unheated wall widths, respectively (see Figure 3).

The expressions developed above for the predicted growth of the stratified layer and the increase in the surface temperature during the stratification process, equations (22) and (34) respectively, are plotted and compared with the results of Tellep and Harper (Reference 4), as well as experimental measurements from this study, in Figures 10 through 13. The numerical calculations used for these comparisons are presented in the Appendix of this report.

EXPERIMENTAL APPARATUS AND PROCEDURE

The vessel used in the experimental program (Figure 5) was made primarily of plexiglass. Two opposite sides each had a one-eighth (1/8) inch thick aluminum sheet inserted approximately three-quarters (3/4) of an inch inward from the plexiglass walls. The aluminum sheet together with the adjacent plexiglass wall created a channel which extended over the entire height and width of the vessel. These channels provided a path through which hot water flowed and consequently heated the alu- minum walls. The top of the vessel was constructed from a combination of wood and Styrofoam which had a high thermal resistance, thereby minimizing the loss of heat and evaporation at the liquid surface. Plexiglass ribs were attached to the channel side of the aluminum sheet. The function of the ribs was to maintain a uniform flow in the vertical direction throughout the channel. Water was used as the test liquid in all of the experiments performed.

For the purpose of fluid temperature data acquisition, a thin wooden post was positioned vertically in the center of the vessel as depicted in Figure 5. The post was attached to the bottom with an adhesive. Chromel-alumel thermocouples were attached at specific inter- vals along the height of the post. With the interior of the vessel filled to a depth of twelve (12) inches with water, the vessel width was six (6) inches and the heated wall width was twelve (12) inches. The uppermost thermocouple was located precisely at the water surface. The remaining thermocouples were located at the following depths below the surface:

FIGURE 5. VESSEL WITH CENTERLINE THERMOCOUPLE POST AND FLOW SEPARATORS

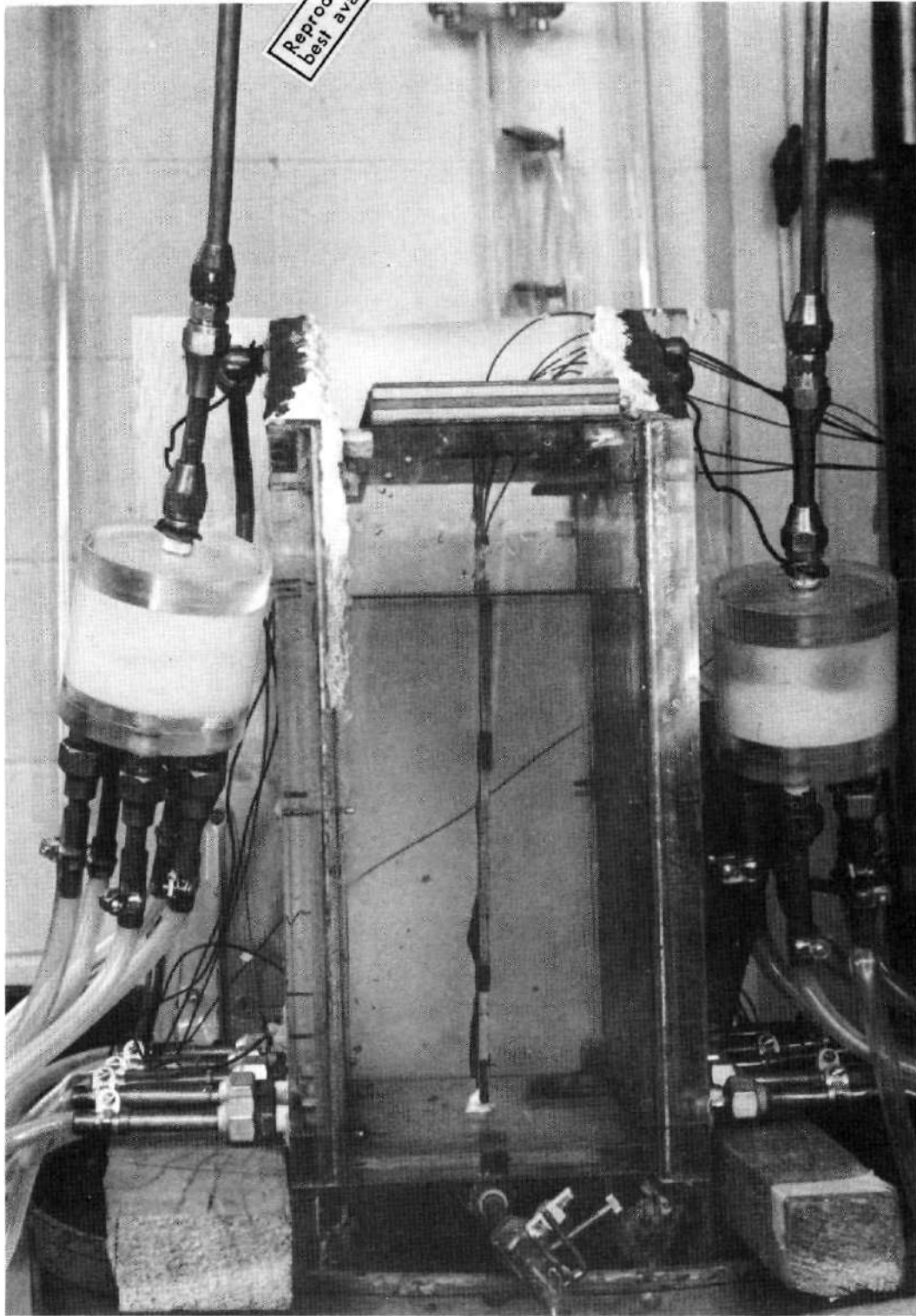FIGURE 5

one-half (0.5) inch, one (1.0) inch, two (2.0) inches, six (6.0) inches,
and eleven (11.0) inches. The reference junction was located in an
ice bath which was maintained at 32 $^\circ$F. A digital voltmeter equipped
with a tape printout system completed the thermocouple circuit. This
instrument is shown in Figure 6. The digital voltmeter (DVM) had the
capability of reading ten (10) inputs sequentially and cyclically.
Each printout consisted of a voltage reading plus the number signifying
the specific thermocouple being read. A complete reading and printing
operation for each thermocouple was performed within an interval of
one second. Other thermocouples were placed at the top and bottom of
the inside and outside of the aluminum walls. These temperatures were
also recorded by the DVM and provided a record for the wall temperatures
throughout each experiment.

The flow through the wall channels originated from a tank of hot
water which was located above the vessel. Flow separators, shown in
Figure 5, had to be inserted in the hot water flow stream between the
source and the vessel channels to insure a proper uniform flow through
the channels. When a valve was suddenly opened to allow the hot water
to flow through the two side channels, the thin aluminum sheets were
heated very rapidly to a temperature just slightly below that of the
hot water. This provided a good approximation to a step change in
wall temperature as far as the interior fluid was concerned.

Experiments were conducted in order to obtain measurements of
some of the important variables in this study, namely, the liquid sur-
face temperature (T_s), the transient centerline temperature distribu-
tion, and the stratified layer thickness (Δ).

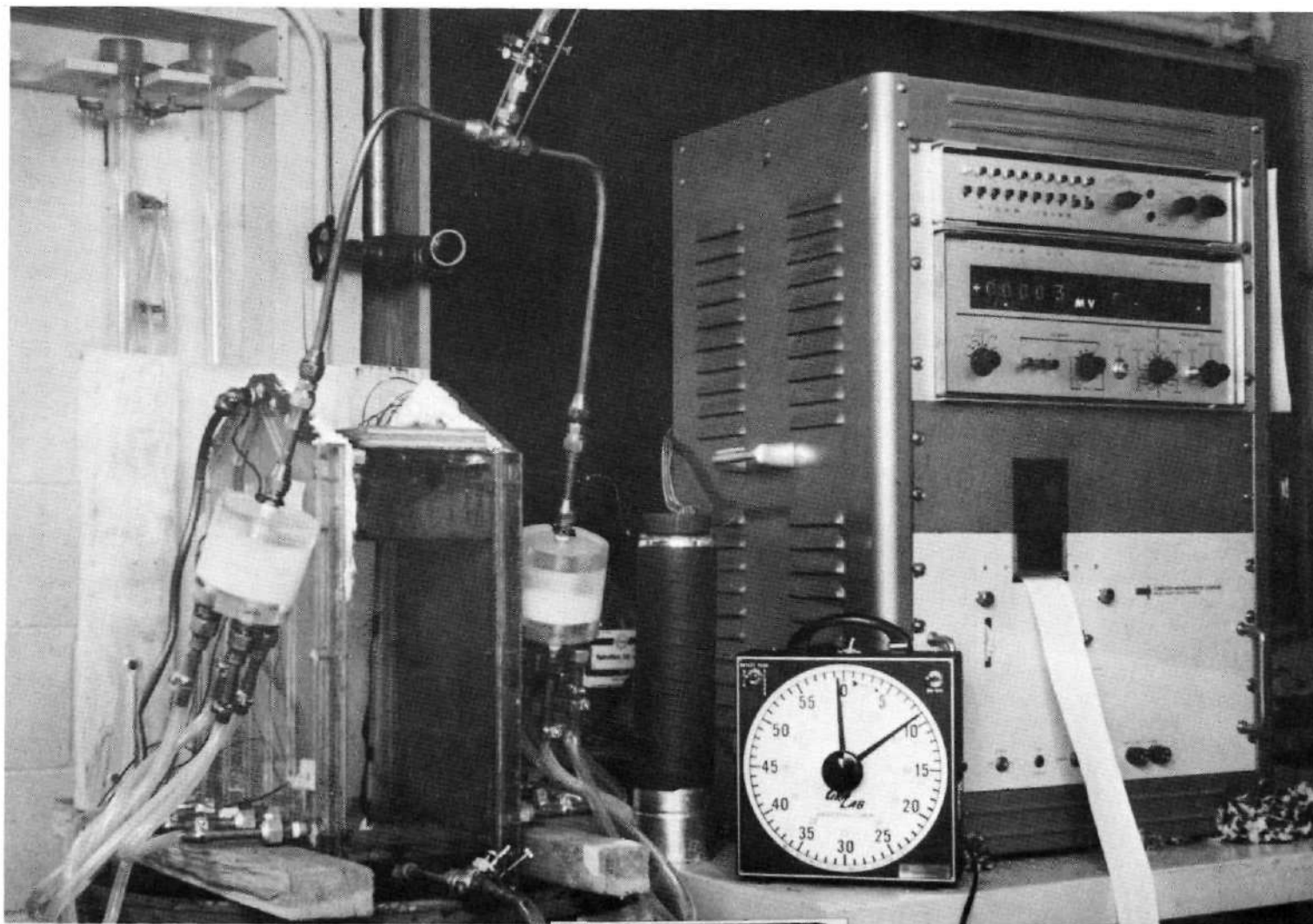FIGURE 6. EXPERIMENTAL APPARATUS COMPLETE WITH AUXILIARY EQUIPMENT

FIGURE 6

Each experiment was initiated by a valve which allowed hot water
to flow through the separators and through the vessel channels along
the two aluminum walls. Heat transfer through the aluminum walls cre-
ated free convection boundary layers along the interior walls, thus
initiating the stratification process. The hot water source was thermo-
statically controlled and the hot water temperature was measured at
the entrance to each channel.

The centerline post, shown in Figure 5, held six (6) thermo-
couples, including the one at the surface. This surface thermocouple
was used to obtain measurements of T_s. The DVM system printed out
values of the surface temperature, as well as the other temperatures
along the vertical centerline, as indicated by the various thermocouples.
The data was converted from millivolts to degrees Fahrenheit. Each
measurement was made dimensionless by subtracting the bulk temperature
(T_b) from it, and then dividing this result by the temperature differ-
ence ($T_w - T_b$). Plots of the resulting measurements, obtained with
several of the thermocouples, are given in the next section of this
report. The increase in the stratified layer thickness (Δ) was deter-
mined by the initial change in each thermocouple reading. Thus, the
downward propagation of the stratified layer, as observed experimentally,
is presented.

The stratification process was also observed by means of a blue
dye. The dye mixture consisted of iodine, water, and starch and had
a specific gravity of 1.015. The dye was introduced into the bulk
fluid, where time was allowed for it to settle to the bottom and to
reach the same temperature as that of the bulk fluid (T_b), before each
observation was initiated. Note that the dye was slightly heavier

than water. This condition was chosen so that the dye would descend
to the bottom prior to each visual test, so that it would clearly show
the upward movement of the fluid once the transient heating process
was initiated. The dye settled on the bottom with a thickness somewhat
less than an inch. Consequently, the dye contacted the boundary layer
near its point of initiation on the wall. Unfortunately, at this loca-
tion the boundary layer was laminar with a very small velocity and was
unable to raise the dye for the lower temperature differences. Only
for the largest temperature differences used (T_w-T_b) was there a suffi-
cient flow which was capable of raising the dye. This condition implies
that the dye flow did not coincide with the front of the stratification
process. In fact, in comparing the centerline thermocouple readings
with the dye flow, it became clear that the dye followed significantly
behind the stratification front. Nevertheless, the dye flow provided
a clear means by which the formation of the stratified layer, as illus-
trated in Figure 2, could be observed.

The dye flow was observed with a television camera and recorded
on a video tape recorder. A clock (Figure 6) was also in the video
picture. It provided an account of the elapsed time as the dye flowed
up the boundary layer and into the stratified layer. Through playback
of the video tape, the mixing occurring within the stratified layer
could be observed as many times as desired. Later in the experimental
program a motion picture camera was substituted for the television
system. This was done to provide a lasting account of the process.
Plus X negative film was used with the camera which was set at sixteen
(16) frames per second.

The two hot water temperatures used were 140 and 180 °F. Thermo-couples were positioned at the bottom and top on both the inside and outside of the aluminum walls. With these thermocouples the actual wall temperature gradients were recorded throughout the experiment. The minimum elapsed time for all of the experiments was eight (8) minutes. This allowed time for each of the six (6) thermocouples to record several temperature values which provided enough plotted data points so that fairly smooth curves could be drawn through them.

RESULTS

Typical data obtained with the thermocouples, employed as described in the preceding section, are presented in Figures 7 and 8 for the centerline temperatures in the fluid. The surface temperature (T_s) lags momentarily, rises rapidly, and then increases at a smoothly decreasing rate while asymptotically approaching the value of the inside wall temperature (T_w). Experiments were conducted at two different values of the temperature difference, and its effect can be evaluated by comparing Figures 7 and 8. A comparison shows that the higher temperature difference causes the centerline temperatures to increase more rapidly to an asymptotic value. The higher temperature difference (Figure 8) shows a greater increase in the centerline temperatures at the depths of one (1.0) and six (6.0) inches. This latter result indicates the increase in the rate of growth of the stratified layer for the higher temperature difference compared to the growth existing at the lower temperature difference. Figure 9 contains plots of the centerline temperature as a function of depth at three different times. The total depth of the fluid was twelve (12) inches. The data show that it took approximately two (2) minutes before the centerline temperature began to increase at three-quarters (3/4) of the total depth.

The analytical predictions formulated in this study for the growth of the stratified layer thickness (equation 22) and the rate of increase of the surface temperature (equation 34) are compared with typical

experimental data and with Tellep and Harper's analytical results in Figures 10 through 13. The numerical calculations associated with the analytical expressions involved are contained in the Appendix. The analytical prediction for the growth of the stratified layer thickness, as displayed in Figures 10 and 11, compares quite favorably with the experimental measurements. The data points shown were obtained by noting the time of the initial increase in temperature for each of the centerline thermocouples which were located at specific depths below the surface. The analytical prediction lies below the data during the first thirty (30) seconds of the stratification process and is somewhat higher thereafter. The analytical prediction of Tellep and Harper (Reference 4) falls below both the experimental data and the analytical prediction of the present study over the entire range of elapsed time shown in Figures 10 and 11. However, the general shape of the curve, including the variation of its slope with time, compares well with both the experimental data and the analytical prediction obtained in this study. The measured results show that about 80% of the twelve (12) inch depth of fluid was stratified after only two (2) minutes had elapsed. The curves of Figure 11 relate the stratified layer thickness to dimensionless time, and therefore, to fluid and container parameters.

An analytical prediction of the surface temperature (T_s) increase during the stratification process is shown for comparison with some typical measurements in Figures 12 and 13. The order of magnitude of the prediction correlates very well with the experimental data during the time in which 80% of the contained fluid is being stratified. However, it can be seen that the predicted surface temperature variation has a discontinuity at t=0. Obviously this is not realistic, as indicated

by the smoothly increasing trend observed experimentally, and is due to
the neglect of the boundary layer inertia (assumption 6) in the analysis.
It can also be seen that after two (2) minutes have elapsed, the analytical
prediction rapidly diverges from the experimental curve. This result can be
attributed largely to the assumptions used in the derivation of equation
(34), particularly assumption 1 which implies a constant heat transfer
rate. This becomes unrealistic as the stratified layer approaches the
bottom of the container. Note that equation (34) states the surface
temperature rate of increase is directly affected by the growth of the
stratified layer thickness during the entire stratification process.
The experimental data, on the other hand, show that after about 80%
stratification has occurred, the surface temperature changes very little
with further elapsed time.

Tellep and Harper's analytical prediction for the surface temperature
increase is also shown in Figure 12 and 13. It can be seen that their
prediction does not correlate well with the experimental data from this
work in the early portion of the transient region, but does become
approximately coincident with the measurements in the 80 to 90% stratification
range. Beyond this range their prediction lies well above the experimental
data points, but the divergence from the experimental results in the latter
portion of the transient period is only about one half as large as the
deviation exhibited by the analytical prediction of the present study.
It should be noted that the analytical predictions of the surface temperatures
should logically lie above the measured data for large times, since both
analyses incorporate the assumption of a constant heat transfer rate,
whereas, the measured data were obtained with essentially a constant wall
temperature condition leading to an actual heat transfer rate which
eventually decreases considerably as the elapsed time increases.

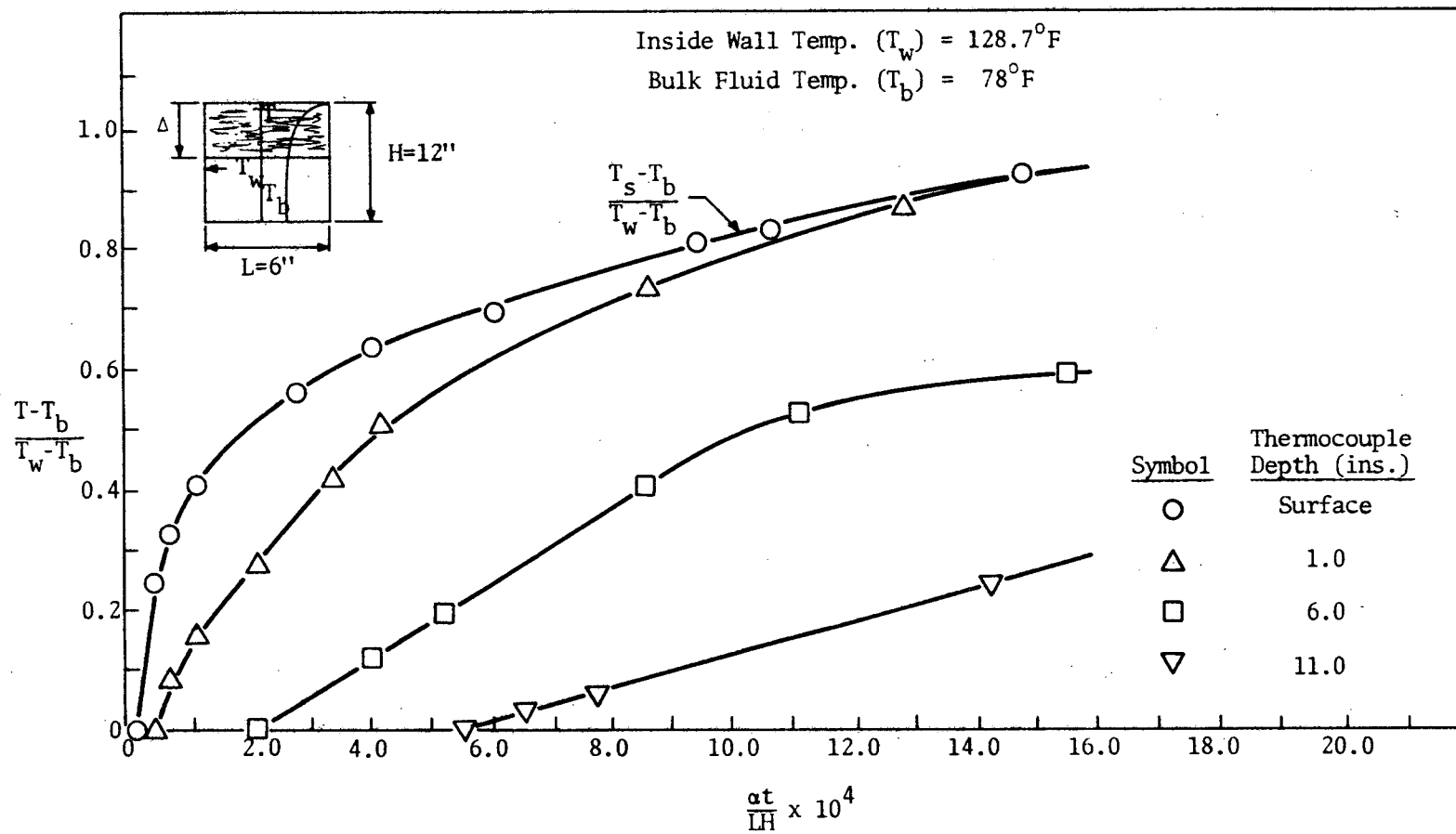FIGURE 7. OBSERVED TEMPERATURE CHANGE AT DIFFERENT DEPTHS WITHIN THE STRATIFIED LAYER ($T_w - T_b = 50.7°F$)
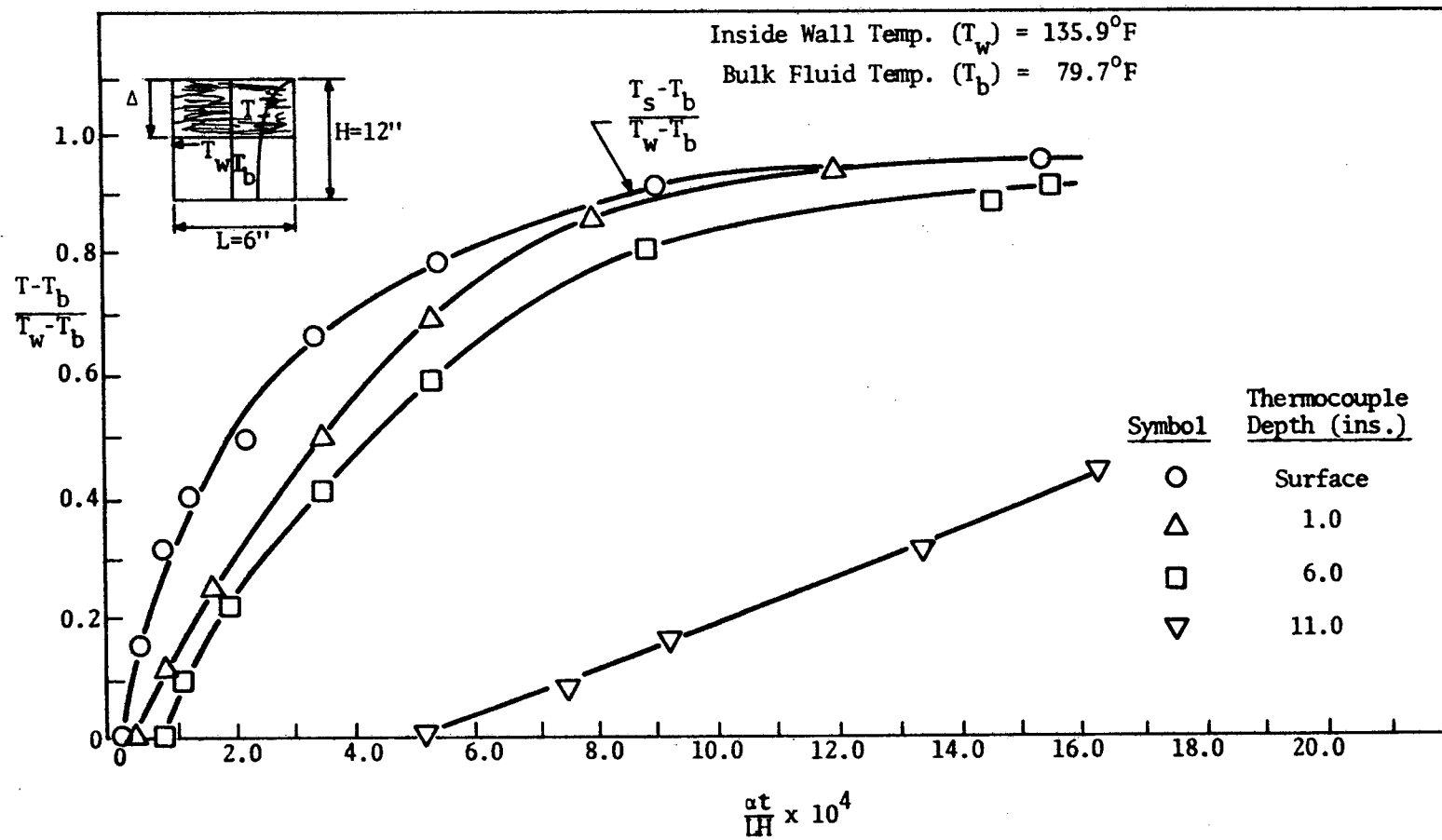
FIGURE 8. OBSERVED TEMPERATURE CHANGE AT DIFFERENT DEPTHS WITHIN THE STRATIFIED LAYER (T_w-T_b = 56.2°F)
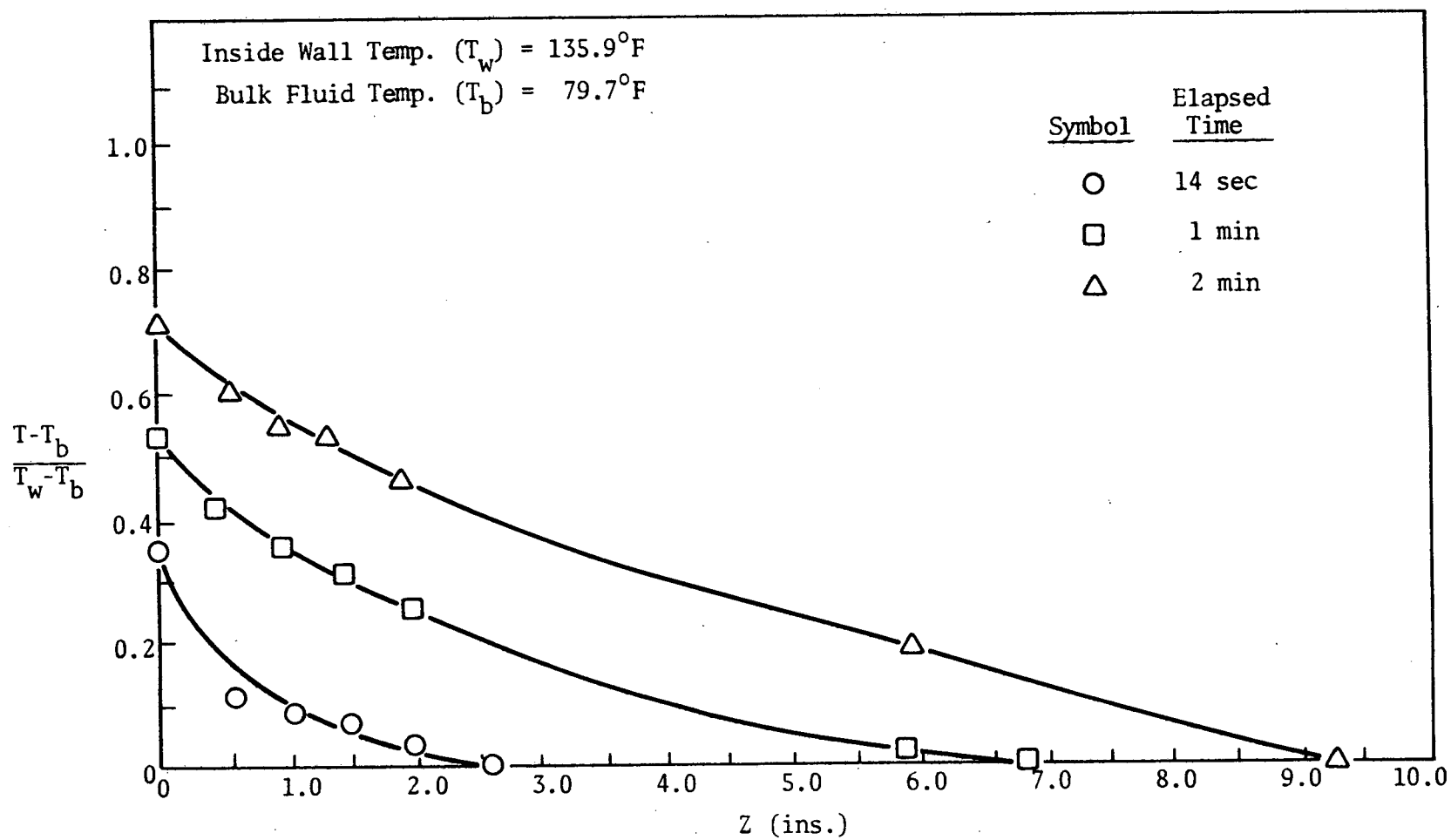
FIGURE 9. OBSERVED TEMPERATURE PROFILES ALONG THE VERTICAL CENTERLINE (T_w-T_b = 56.2°F)

FIGURE 10. COMPARISON OF ANALYTICAL AND EXPERIMENTAL RESULTS FOR THE STRATIFIED LAYER GROWTH

Legend:

—△— Experimental Data
(From ¢ Temp. Increase)
$T_w = 135.9°F$ $T_b = 79.7°F$

----- Tellep & Harper
(Analytical)

—— Present Analysis (Eqn. 22)

$\frac{\Delta}{H}$ (y-axis)

$\frac{\alpha t}{LH} \times 10^4$ (x-axis)

FIGURE 11. COMPARISON OF ANALYTICAL AND EXPERIMENTAL RESULTS FOR THE STRATIFIED LAYER GROWTH

FIGURE 12. COMPARISON OF ANALYTICAL AND EXPERIMENTAL RESULTS FOR SURFACE TEMPERATURE INCREASE

FIGURE 13. COMPARISON OF ANALYTICAL AND EXPERIMENTAL RESULTS FOR SURFACE TEMPERATURE INCREASE

CONCLUSIONS

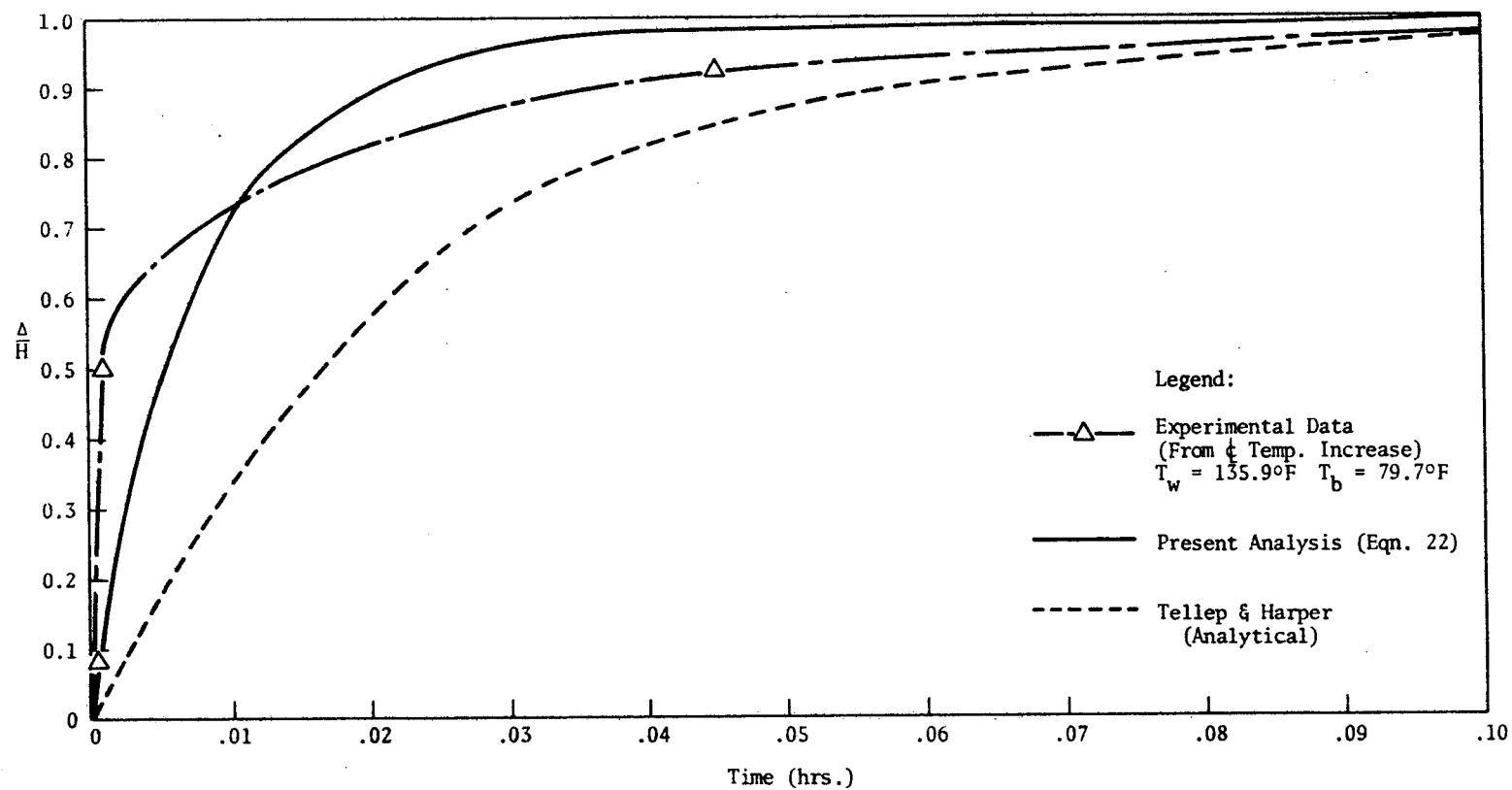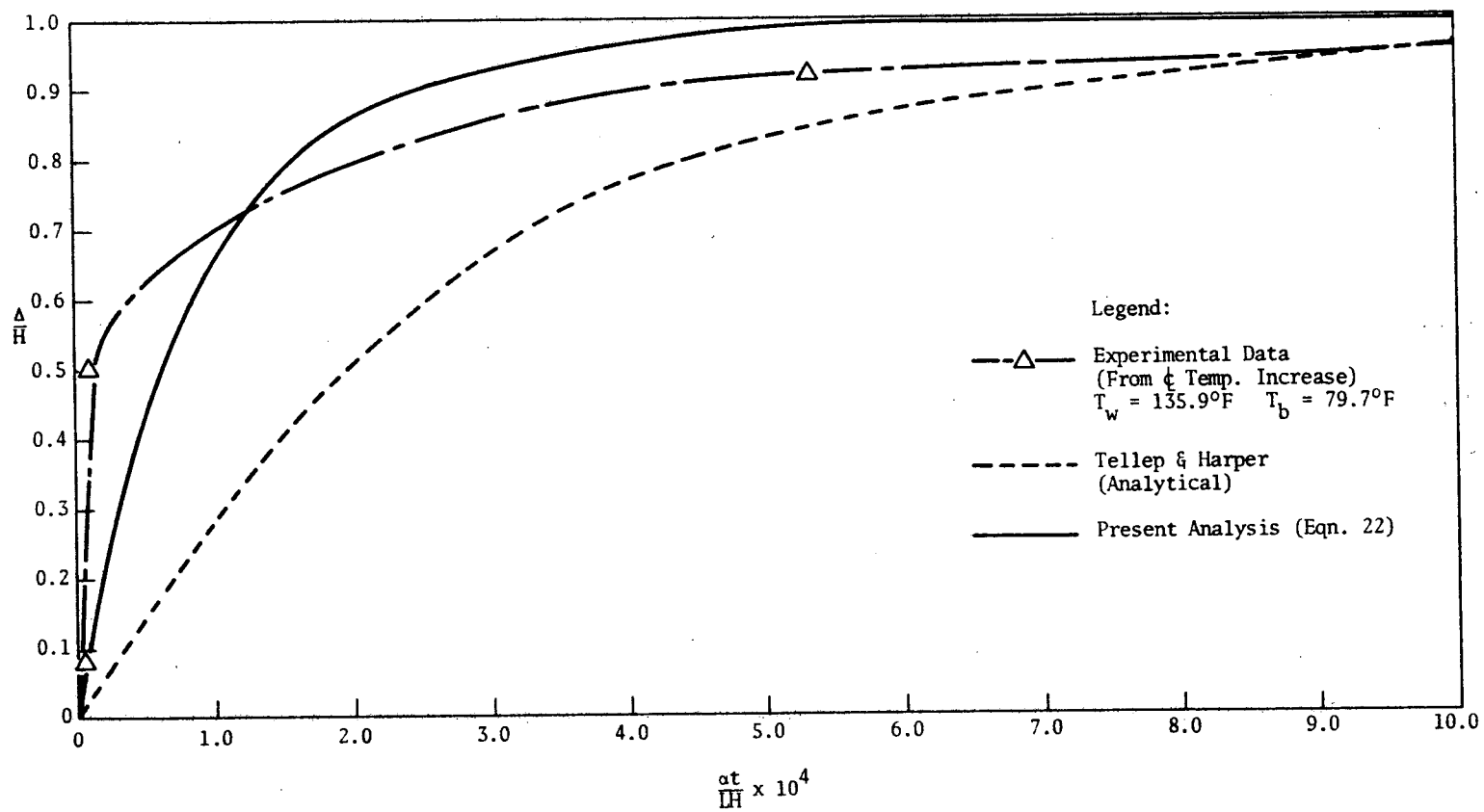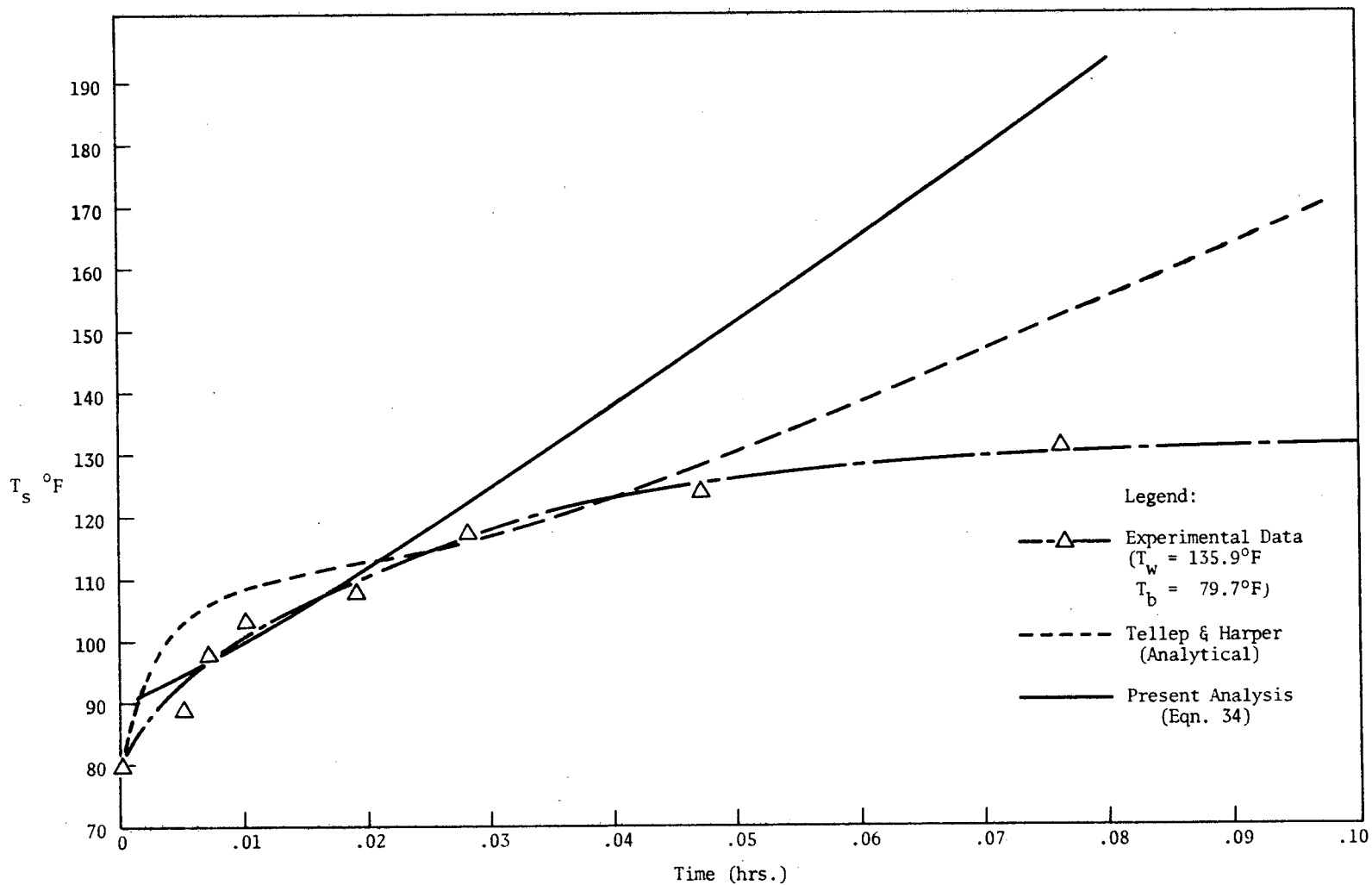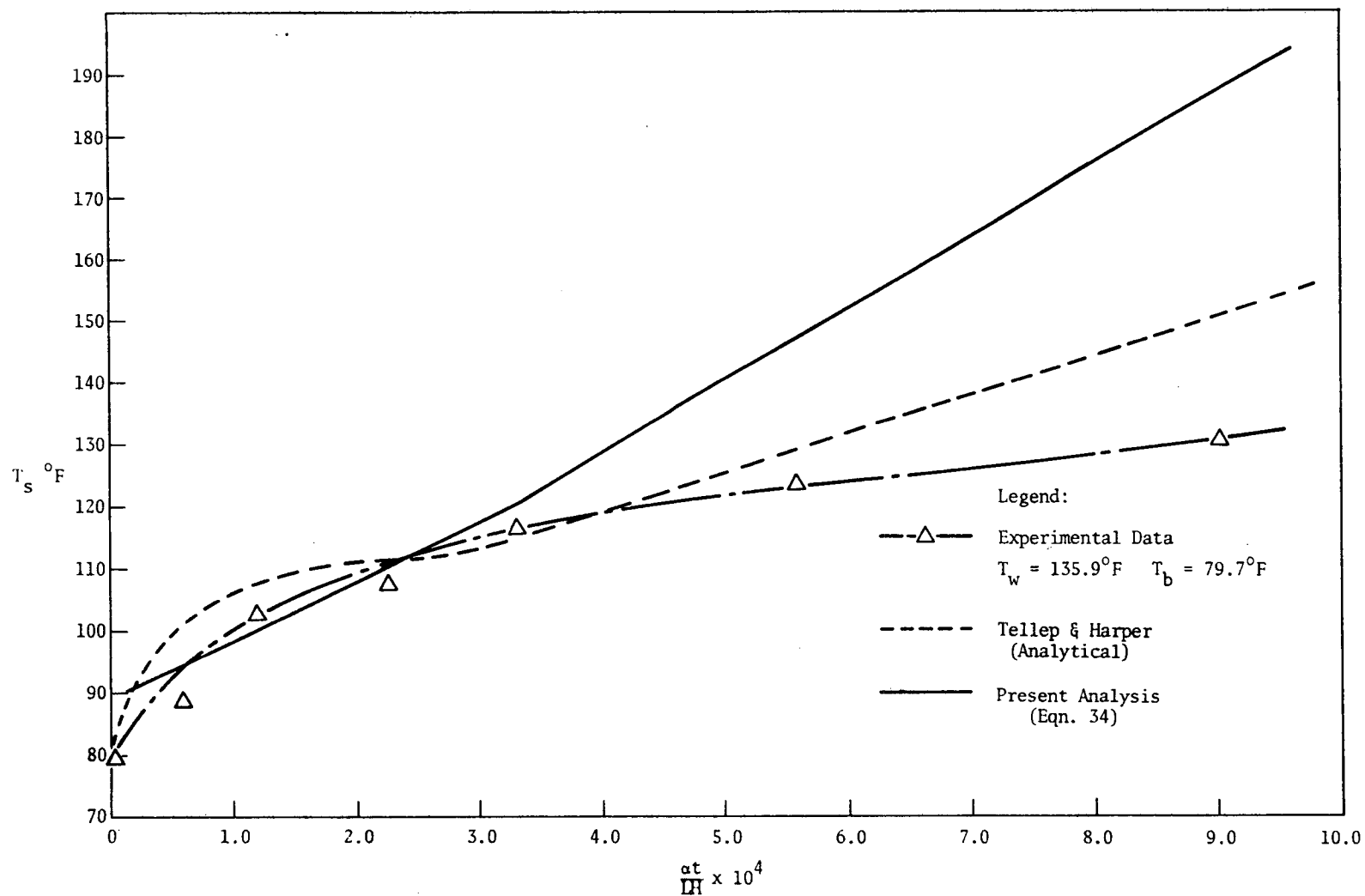This study has involved an analytical and experimental investigation of the transient stratification of water contained in a rectangular vessel. It is concluded that the stratification of a contained fluid with side wall heating due to a constant temperature can be approximately predicted by means of an analysis based on a simplified physical model. A summary of the pertinent results is given below:

1. An analysis based on fundamental heat transfer equations produced an expression which predicted approximately the growth of the stratified layer. This was confirmed experimentally by observing the times at which the various center-line temperatures first began to increase.

2. The same analysis yielded an expression for the increase of the surface temperature which compared favorably with experimental data during the early portion of the transient period, but which was found to overpredict the surface temperature during the latter portion of the transient period.

3. The dimensionless results indicate the manner in which the fluid properties and vessel geometry affect the stratification process.

LIST OF REFERENCES

LIST OF REFERENCES

1. L.E. Scott, R. Robbins, D. Mann, and B. Birmingham, "Temperature Stratification in a Nonventing Liquid Helium Dewar," Journal of Research of the National Bureau of Standards, Vol. 64C, No. 1, pp. 19-23, January-March, 1960.

2. B.N. Anderson, S. Huntley, and D. Connolly, "Propellant Heating Studies with Wall and Nuclear Heating," ASME Publication, 64-WA/AV-8, September, 1964.

3. H.Z. Barakat, "Transient Laminar Free-Convection Heat and Mass Transfer in Two-Dimensional Closed Containers Containing Distributed Heat Source," ASME Publication, 65-WA/HT-28, July, 1965.

4. D.M. Tellep and E. Harper, "Approximate Analysis of Propellant Stratification," AIAA Journal, Vol. 1, No. 8, pp. 1953-56, August, 1963.

5. J.M. Ruder, "Stratification in a Pressurized Container with Sidewall Heating," AIAA Journal, Vol. 3, pp. 135-137, January, 1964.

6. E.R.G. Eckert and Thomas W. Jackson, "Analysis of Turbulent Free-Convection Boundary Layer on a Flat Plate," NACA Journal, Report 1015, pp. 1-7, July, 1950.

7. R.G. Schwind and G.C. Vleit, "Observations and Interpretations of Natural Convection and Stratification in Vessels," Proc. of the 1964 Heat Transfer and Fluid Mechanics Institute, Stanford University Press, pp. 51-68, 1964.

8. Edward E. Duke, "Nuclear Heating and Propellant Stratification," AIAA Journal, Vol. 3, No. 4, p. 760, April 1965.

9. T. Bailey, R. VandeKoppel, G. Skartvedt, T. Jefferson, "Cryogenic Propellant Stratification Analysis and Test Data Correlation," AIAA Journal, pp. 1657-58, July, 1963.

10. S.W. Churchill, "The Prediction of Natural Convection," Third International Heat Conference.

11. F. Kreith, "Principles of Heat Transfer," International Textbook Company.

Additional References

1. Papers from Proceedings of the Conference on Propellant Tank Pressurization and Stratification, NASA, George C. Marshall, Space Flight Center, Huntsville, Alabama, January 20-21, 1965.

2. J.A. Tatom, W.H. Brown, L.H. Knight, and E.F. Core, "Analysis of Thermal Stratification of Liquid Hydrogen in Rocket Propellant Tanks," Advances in Cryogenic Engineering, Vol. 9, pp. 254-264. 1963.

3. M. Segel, "Experimental Studies of Stratification Phenomena and Pressurization for Liquid Hydrogen," Cryogenic Engineering Conference, Philadelphia, August, 1964.

APPENDIX

APPENDIX

NUMERICAL CALCULATIONS

In this section the analytical expressions will be utilized for a specific condition. The temperature difference $(T_w - T_b)$ to be investigated is

$$(T_w - T_b) = 135.9 \ ^oF - 79.7 \ ^oF = \underline{56.2 \ ^oF}.$$

The parameters will be evaluated at the average temperature

$$\bar{T} = \frac{T_w + T_b}{2} = \underline{107 \ ^oF}.$$

The tables in Reference 11 provide the following values:

$$Pr = 4.52, \ \beta = 0.219 \times 10^{-3}/^oF, \ \nu = 0.692 \times 10^{-5} \ ft^2/sec.$$

The known parameters are,

$$P = 1 \ ft, \ g = 32.2 \ ft/sec^2, \ A_s = 1/2 \ ft^2, \ L = 1/2 \ ft, \ H = 1 \ ft.$$

Let's recall equation (22),

$$\frac{\Delta}{H} = 1 - \left\{ 1 + .0338 \ \nu \left(\frac{P}{A_s}\right) (Pr)^{8/15} \left[\frac{g\beta \ (T_w - T_b)}{\nu^2}\right]^{2/5} \right.$$
$$\left. \left[1 + .494 \ (Pr)^{2/3}\right]^{-2/5} H^{1/5} t \right\}^{-5}$$

which after termwise exponentiation becomes,

$$\frac{\Delta}{H} = 1 - \left\{ 1 + .0388 \left[\frac{2}{ft}\right] \left[0.692 \times 10^{-5} \frac{ft^2}{sec}\right] (2.24) \left[.926 \times 10^4/ft^{6/5}\right]\right.$$
$$\left. [1 + .494 (2.738)]^{-2/5} (ft^{1/5}) \ t(hr) \right\}^{-5}$$

This expression reduces to

$$\frac{\Delta}{H} = 1 - \left\{ 1 + 28.44 \frac{t}{hr} \right\}^{-5}$$

$\frac{\Delta}{H}$ values can be obtained by substituting time in hours for t. The following values result.

t (hr)	28.44 t	1 + 28.44 t	$(1 + 28.44 \ t)^{-5}$	Δ/H
0	0	1	1	0
.001	.028	1.028	.872	0.128
.005	.142	1.142	.516	0.484
.010	.284	1.284	.288	0.712
.015	.427	1.427	.170	0.830
.020	.569	1.569	.106	0.894
.040	1.138	2.138	.023	0.977
.050	1.422	2.422	.012	0.988
.060	1.706	2.706	.007	0.993
.080	2.275	3.275	.003	0.997
.100	2.844	3.844	.001	0.999

The values for $\frac{\Delta}{H}$ from this table are plotted and compared with Tellep and Harper's results, and experimental data from this work, in Figure 10.

The calculations continue by employing equation (34) to obtain the analytical rate of increase of the surface temperature (T_s) for the same specific condition used to obtain (Δ) in the preceding calculations. The surface temperature increase is predicted by equation (34),

$$\frac{T_s - T_b}{T_w - T_b} = $$

$$\frac{\left(\frac{6\bar{h}}{\rho L c}\right) t}{\left\{1 - \left[1 + .0388 \, \nu \left(\frac{P}{A_s}\right) (Pr)^{8/15} \left[\frac{g\beta(T_w - T_b)}{\nu^2}\right]^{2/5} \left[1 + .494(Pr)^{2/3}\right]^{-2/5} H^{1/5} t\right]^{-5}\right\}}$$

The heat transfer coefficient $\bar{h}$ will be calculated using the expression for turbulent flow given in the analysis as equation (1). Thus,

$$\bar{h} = 0.021 \, \frac{k_f}{H} (GrPr)^{2/5}$$

where

$$Pr = 4.52$$

$$Gr = \frac{g\beta(T_w - T_b)H^3}{\nu^2} = 825 \times 10^7$$

$$k_f = 0.363 \, \frac{Btu}{hr\text{-}ft \, ^\circ F}$$

and

$$\bar{h} = .021 \, (.363) \left[(825 \times 10^7)(4.52)\right]^{2/5} \frac{Btu}{hr\text{-}ft^2 \, ^\circ F}$$

$$\bar{h} = \underline{129.0} \, \frac{Btu}{hr\text{-}ft^2 \, ^\circ F}$$

The constant term in the numerator can be calculated,

$$\frac{6\bar{h}}{\rho L c} = \underline{25.048/hr}$$

which is substituted into equation (34) along with Δ/H for the denomi-nator. Thus,

$$\frac{T_s - T_b}{T_w - T_b} = \frac{25.048 \frac{t}{hr}}{\frac{\Delta}{H}}$$

The values for T_s can be found by substituting time in hours for (t) and the corresponding values for $\frac{\Delta}{H}$ from the preceding table.

t (hr)	Δ/H	$T_s - T_b$	T_s °F	$\frac{\alpha t}{LH} \times 10^4$
.001	.128	10.96	90.66	.118
.005	.484	14.54	94.24	.593
.010	.712	19.77	99.47	1.186
.015	.830	25.44	105.14	1.779
.020	.894	31.49	111.19	2.372
.040	.977	57.62	137.32	4.744
.050	.988	71.26	150.96	5.930
.060	.993	85.04	164.74	7.116
.080	.997	112.92	192.62	9.488
.100	.999	140.94	220.64	11.860

These data are plotted and compared in Figure 12.

Since Tellep and Harper's work (Reference 4) played a very important part in the analysis, the results, both analytical and experimental, were compared with their data in Figures 10 through 13. It must be

understood that their work was conducted in a cylindrical container as compared to the rectangular container used in this work. This conflict was considered and it was reasoned that the radius of the circumscribed circle of a square using P = 1 ft as a side would be an approximation to the radius of the cylindrical container (R). Therefore, since the length of a radius of a circumscribing circle is 3/4 of the length of a side, the following relation was used: R = 3/4, P = 1 ft. This value of R was substituted into Tellep and Harper's turbulent prediction, namely,

$$\frac{\Delta}{H} = 1 - \left[1 + .082 \ (H/R) \ (Gr*/Pr)^{2/7} \ \phi\right]^{-7}$$

where

$$\phi = \frac{\nu t}{H^2}$$

$$Gr* = \frac{g \beta \dot{q} H^4}{k_f \nu^2} \quad (\dot{q} \equiv \text{wall heat flux})$$

The wall heat flux ($\dot{q}$) was determined using the temperature difference ($T_w - T_b$) incorporated in the previous calculations. Thus,

$$\dot{q} = \bar{h} \ (T_w - T_b) = \text{constant (Reference 4)}$$

$$\dot{q} = (129) \ (56.2 \ ^\circ F) = 7249.8 \ \frac{Btu}{hr\text{-}ft^2}$$

and

$$Gr* = 293.8 \times 10^{10}, \ Pr = 4.52$$

$$\phi = .025 \ (t \ hr)$$

Values for $\frac{\Delta}{H}$ can now be found by the following procedure:

(1) Value from Figure 2 (Reference 4) $= \frac{H}{R} \left[\frac{Gr*}{Pr}\right]^{2/7} \phi$

or $t(hr) = \frac{\text{Figure 2 value}}{77.7}$

(2) With t known, $\frac{\Delta}{H}$ can be calculated

t(hr)	Δ/H
0	0
.0032	0.110
.0064	0.215
.0129	0.410
.0193	0.560
.0257	0.670
.0515	0.870
.0772	0.940
.1030	0.975

These values are plotted in Figure 10.

A comparison was also made with Tellep and Harper's surface temperature increase results. Their turbulent prediction is,

$$\frac{T_s - T_b}{\dot{q} \, H/k_f} = \frac{2 \, (H/R) \, \phi}{I \, Pr \, \{1 - [\Delta/H]\}}$$

where I is an energy integral representing the average temperature rise in the stratified layer. They suggest a value of 0.33 which was used to plot T_s. The following table gives the values used to plot T_s vs time in Figure 12.

t(hr)	$T_s - T_b$	T_s °F	$\frac{\alpha t}{LH} \times 10^4$
0	0	79.7	0
.0064	23.97	103.7	.76
.0129	29.96	109.7	1.53
.0193	31.95	111.7	2.29
.0257	33.95	113.7	3.05
.0386	43.94	123.6	4.58
.0515	51.92	131.6	6.11
.0772	71.90	151.6	9.16
.1030	93.86	173.6	12.22

SECTION 2

AN INTERFEROMETRIC STUDY OF THERMAL STRATIFICATION

BY NATURAL CONVECTION IN A CONTAINED LIQUID[1]

o

AN INTERFEROMETRIC STUDY OF THERMAL

STRATIFICATION BY NATURAL CONVECTION

IN A CONTAINED LIQUID

R. I. Haug, W. H. Stevenson, E. R. F. Winter

Lafayette, Indiana, U.S.A.

Abstract Transient laminar free convection to water in a rectangular container was investigated using a Mach-Zehnder interferometer. The experimentally observed temperature profiles are compared with analytically predicted profiles based on a computer program developed by Barakat. Good agreement between analysis and experiment was obtained. In addition qualitative observations of the conditions in the container during sudden discharge of the liquid are reported.

Zusammenfassung Untersucht wurde der unstetige, laminare Warmeubergang durch freie Konvektion in Wasser in einem rechteckigen Behalter mittels eines Zehnder-Mach Interferometers. Die im Experiment beobachteten Tem- peraturprofile wurden mit den analytisch vorausgesagten Profilen verglichen, die mit einem Komputerprogramm, das von Barakat entwickelt wurde, erzielt wurden. Gute Uebereinstimmung zwischen Analyse und Experiment wurde erreicht. Ausserdem werden qualitative Beobachtungen der Vorgange im Behalter wahrend des plotzlichen Leerens der stratifizierten Behalter- flussigkeit berichtet.

INTRODUCTION

During the past decade the process of thermal stratification by natural convection heat transfer to contained liquids has been the subject

of numerous analytical and experimental investigations. A review article
by Clark [1] covered research done in this area through 1965. More recent
analytical and experimental work is reported by Barakat [2] and Barakat
and Clark [3], [4]. These latter studies are of particular interest here,
since a complete numerical solution to the momentum and energy equations
was obtained for the laminar flow case without invoking the boundary layer
assumptions. The predicted temperature field near the heated vertical
walls was found to differ markedly from that developed in an unconfined
fluid. A prime objective of the present investigation was to experimentally
verify this behavior using a Mach-Zehnder interferometer. This experi-
mental technique also allowed certain other aspects of the stratification
process to be observed qualitatively, including the temperature distri-
bution in the liquid during discharge from the container.

Since the stratification phenomenon is so well documented, only a
brief discussion of important considerations in the present study is
necessary here. The governing equations for this problem are the x and y
momentum equation, the continuity equation, and the energy equation. A
computer solution of these equations was obtained by Barakat after first
transforming the momentum and continuity equations into dimensionless
expressions in terms of the stream function and the vorticity. Details
of this transformation may be found in the publications by Barakat and
Clark [2], [3], and [4]. The computer program given in [2] was modified
slightly and used by the authors as a basis for comparison of experimental
results with analytical predictions.

To aid in the explanation of essential features of the problem the
important assumptions made in the analysis are presented here.

The following thermal boundary conditions were used:

(1)   The bottom surface of the container and the free surface of the liquid are perfectly insulated.

(2)   The liquid in the container is initially at a uniform temperature T_o.

(3)   Starting at time zero the wall temperature T_w (assumed to be uniform with location) is increased in some prescribed manner to a final steady value, $T_w (\infty)$.

The boundary and initial conditions for the momentum equation are listed below:

(1)   No slip exists at the wall.

(2)   The shear at the free surface is zero.

(3)   The velocity is initially everywhere zero in the container.

In addition to the above conditions, several other simplifying assumptions were made. The dissipation term in the energy equation was assumed negligible. Flow was assumed to be laminar and incompressible at all times and the process was taken to be two-dimensional. Also all fluid properties were assumed constant with the exception of the density in the body force term of the momentum equation which was allowed to vary with temperature.

EXPERIMENTAL APPARATUS

A Mach-Zehnder interferometer with a helium-neon laser source was employed to obtain data on temperature profiles in the contained liquid. The use of a laser eliminated the need for a compensating chamber in the reference path of the interferometer. (A good discussion of the use of

a compensating chamber is presented by Goldstein and Eckert [5], who used an interferometer to study transient free convection from a vertical plate in water. Another interferometric study pertinent to the present experiment was the investigation of laminar free convection heat transfer in a liquid with internal heat generation carried out by Novotny and Eckert [6].)

Figure 1 shows the test apparatus used in this study. It consisted of two independent units - a Plexiglass container with optical glass end windows to hold the liquid and a separate heating section which was inserted into the container. In order to permit observation of phenomena occurring during discharge, a rotary Teflon valve was designed and installed in the test section base. When opened this valve allowed the liquid to be discharged through an unobstructed 1.6 mm wide slot. The heating section was also constructed primarily of Plexiglass. Aluminum plates were bonded to the inner vertical surfaces which had channels milled in them for water passage. These channels were connected to a water circulator and temperature control bath. In operation, therefore, the exposed surfaces of the aluminum plates attained a uniform temperature very close to that of the circulating water, which was thermostatically controlled to $\pm$ 0.1°C.

Temperature measurements for reference purposes were made with four copper-constantan thermocouples. Two of these were used to monitor the temperature in the bulk liquid near the bottom of the test section. The remaining thermocouples were placed in one of the aluminum plates at two different heights to permit confirmation of the temperature uniformity and measurement of the initial wall temperature transient. During a normal run, the aluminum side plates rapidly approached their steady state temperature after introduction of water from the circulator into the

heating passages. The time constant for a 5°C wall temperature rise was approximately five seconds. The actual recorded variation with time was used as a boundary condition in the computer analysis.

RESULTS

Experimental data were obtained for values of $T_w(\infty) - T_o$ ranging up to 7°C. These data were extracted from infinite fringe interferograms such as the typical one shown in Fig. 2. A complete set of such photographs taken at intervals after the start of heating provides a detailed picture of the entire stratification process. One qualitative observation of some importance is the intense turbulent mixing action which occurs early in the process when the two streams of heated liquid moving along the free surface first merge at the center of the container. Laminar conditions were re-established fairly rapidly, but the temperature and flow fields were quite complex during the next few seconds.

A very interesting feature of the stratification process is the temperature reversal in the region near the wall. This is shown clearly in Fig. 2. It can be seen that the temperature initially decreases with distance from the wall and then increases again. This is caused by two effects.

(1) Since the Prandtl number is greater than one, the hydro-dynamic boundary layer is thicker than the thermal layer. Thus cool liquid from the bulk fluid moves upward along with the heated fluid within the thermal boundary layer.

(2) The downward moving stratified liquid in the central region of the container is at a high temperature relative to that

of the upward moving liquid in the unheated portion of
the hydrodynamic boundary layer. Thus the temperature
reversal shown results.

Experimentally determined temperature profiles obtained from one set
of interferograms at three different vertical positions in the container
are shown in Fig. 3, together with calculated results obtained from the
modified computer program. In order to illustrate the region of tempera-
ture reversal clearly, the curves of Fig. 3 are drawn on an expanded
scale. A test duration of two minutes was felt to be about the maximum
over which accurate results could be expected due to heat losses from the
container. At 123 seconds the largest error occurred in the lower portion
of the container. This error (based on the overall temperature difference
between the wall and the bulk liquid) is only 23 percent. The agreement
at other times and positions was much better.

It will be noted that the experimental temperatures are lower than
the computed values in all cases. This is to be expected, since heat
losses were present in the experimental system which were not accounted
for in the analysis. In particular, energy was lost at the free surface
of the liquid by conduction and evaporation, and at the glass end windows
by conduction. The former effect was found to be negligible; an approxi-
mate energy balance indicated that the energy loss to the glass windows
accounted for most of the discrepancy between analysis and experiment.

In addition to the quantitative measurements described, qualitative
observations of the stratified fluid during discharge from the container
were made. This was accomplished by taking movies of the interference
pattern after suddenly opening the discharge valve. It was found that the

discharge process was basically laminar during the early stages with no significant mixing of the liquid. When approximately two thirds of the liquid had been discharged the process changed rapidly and an intense mixing occurred during the final phase.

CONCLUSIONS

The good agreement between analysis and experiment, particularly when the energy losses in the experimental system are taken into account, appears to verify the description of the stratification process provided by the work of Barakat and Clark. One effect present in an actual system which is not accounted for in their analysis is the turbulent mixing which occurs when the two streams of heated fluid first merge. The effect of this on the overall process at later times is obviously a function of the container size and the temperature ratios involved, as well as the fluid properties.
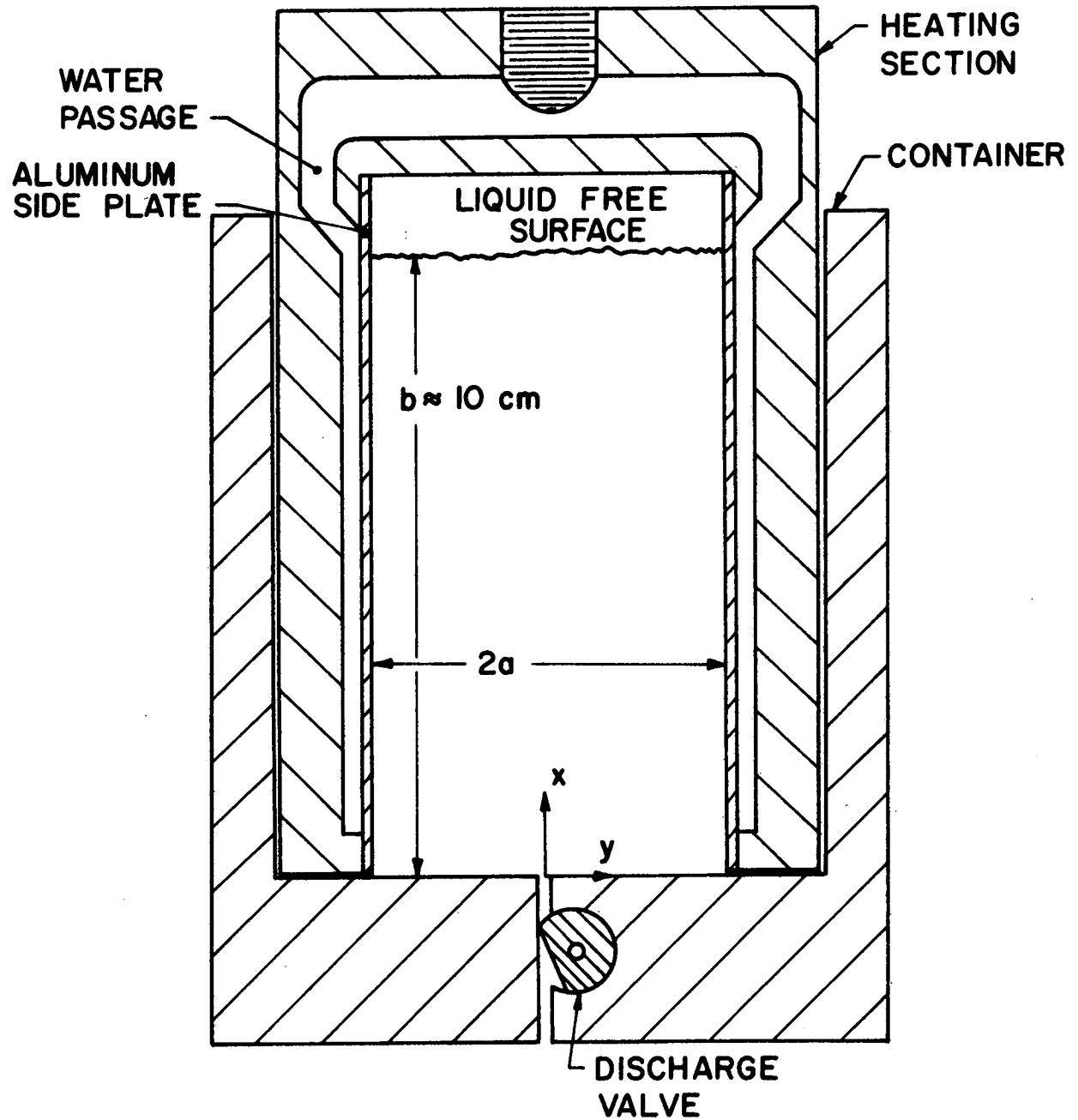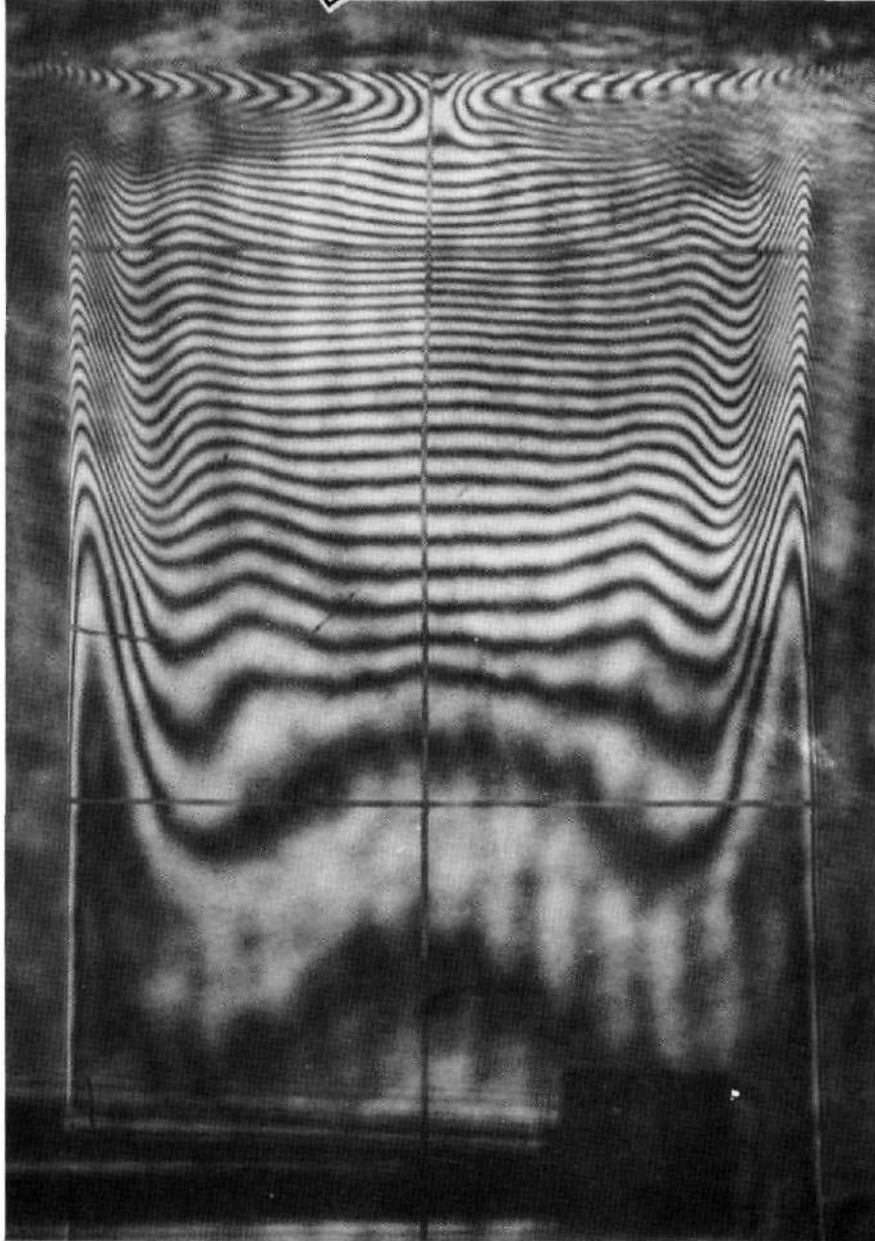
Figure 1. Experimental Test Apparatus

Figure 2. Typical Interferogram

x/b=0.75

123 sec.

87 sec.

45 sec.

1.0 0.8 0.6 0.4 0.2 0.0
y/a

- - - - - CALCULATED
——— OBSERVED

$T_W(\infty) - T_0 = 6.1\ °C$

WATER DEPTH
10.2 cm.

x/b = 0.5

123 sec.

87 sec.

1.0 0.8 0.6 0.4 0.2 0.0
y/a

x/b = 0.25

123 sec.
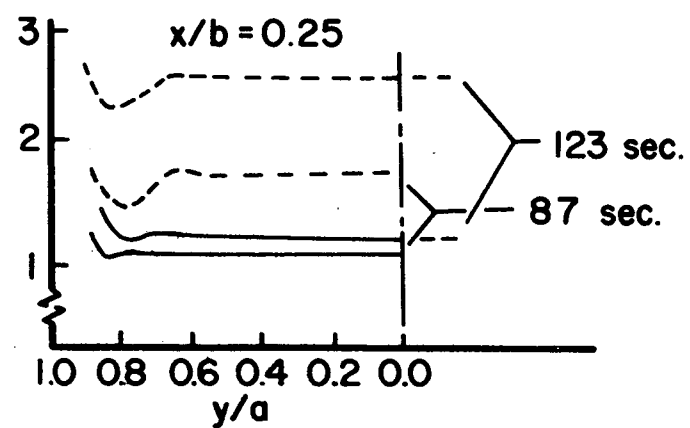
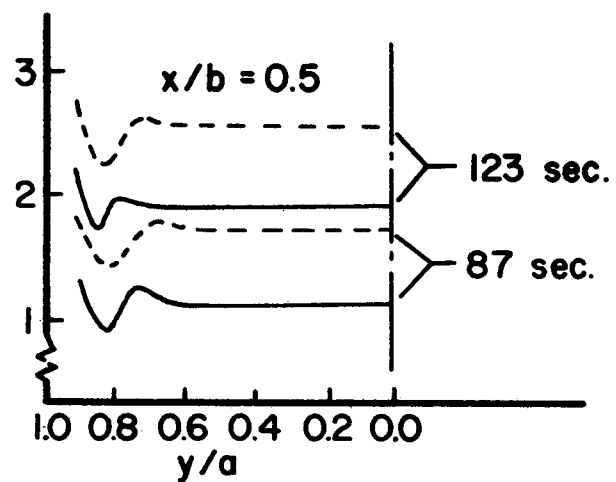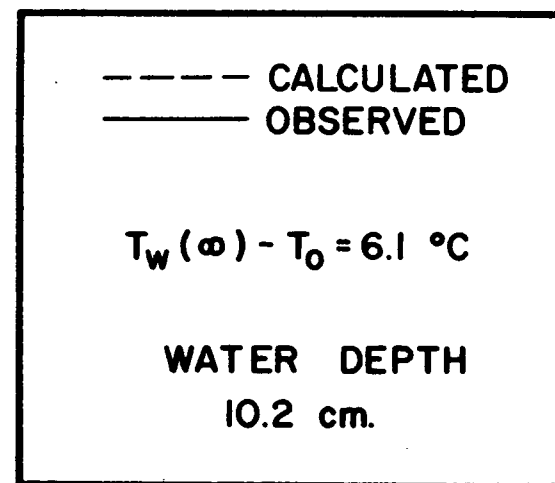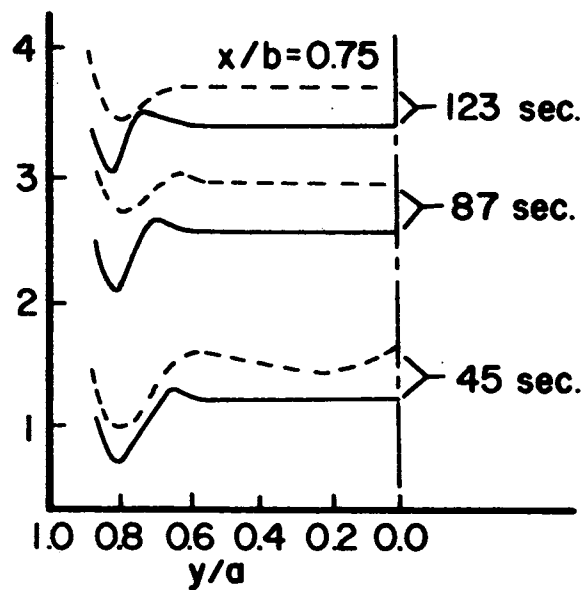87 sec.

1.0 0.8 0.6 0.4 0.2 0.0
y/a

Figure 3.   Experimental Results

REFERENCES

[1] Clark, J. A. "A Review of Pressurization, Stratification, and Interfacial Phenomena," Vol. 10, International Advances in Cryogenic Engineering, pp. 259/289, New York: Plenum Press, 1965.

[2] Barakat, H., "Transient Natural Convection Flow in Closed Containers," Ph.D. Thesis, University of Michigan, 1965.

[3] Barakat, H., and Clark, J. A., "Transient Laminar Free Convection Heat and Mass Transfer in Closed, Partially Filled, Liquid Containers," Technical Reports 1 and 2, Contract NAS-8-825, Huntsville, Alabama, 1965.

[4] Barakat, H. and Clark, J. A., Proceedings of the Third International Heat Transfer Conference, Vol. II (1966), pp. 152/162

[5] Goldstein, R. J., and Eckert, E. R. G., "Int. J. Heat Mass Transfer," Vol. 1 (1960), pp. 208/218.

[6] Novotny, J. T., and Eckert, E. R. G., "Int. J. Heat Mass Transfer," Vol. 7 (1964), pp. 955/968.

R. I. Haug, Prof. W. H. Stevenson and Prof. E. R. F. Winter

School of Mechanical Engineering
Purdue University
Lafayette, Indiana 47907, U.S.A.

Manuskript eingegangen am . . . .

SECTION 3

USE OF MULTIPLE OUTLETS FOR REDUCING THE STRATIFICATION-

INDUCED PROPELLANT SUPPLY TEMPERATURE RISE[1]

USE OF MULTIPLE OUTLETS FOR REDUCING THE
STRATIFICATION-INDUCED PROPELLANT SUPPLY TEMPERATURE RISE

R. J. Schoenhals[*], R. N. Nelson[+], and E. R. F. Winter[*]

Heat transfer to the fuel or oxidizer of a liquid fuel rocket produces thermal stratification, and this typically causes an increase in the propellant supply temperature during the latter portion of the engine burning period when the warmer fluid in the stratified layer is being discharged from the supply tank. This behavior is undesirable because of the potential problem of cavitation in the supply pumps. In this paper a technique is described for reducing the stratification-induced supply temperature rise. Multiple outlets are employed which feed into a mixing chamber below the supply tank. Experimental measurements are presented which illustrate the value of the proposed concept.

INTRODUCTION

During operation of liquid fuel rockets heat is unavoidably transferred to propellant supply tanks containing cryogenic fluids, both prior to and during flight. As the liquid in the boundary layer adjacent to the tank wall is heated, it rises due to buoyancy and is replaced by cooler liquid from the central core (Fig. 1)[‡]. The upward-moving fluid moves radially inward as it approaches the free surface, and then

---

[*] Professor of Mechanical Engineering, School of Mechanical Engineering, Purdue University, Lafayette, Indiana

[+] Ensign, U. S. Navy, Naval Ship Systems Command, Division of Naval Reactors, Washington, D. C.

[‡] Definitions are given at the end of the paper for all symbols appearing in the illustrations and in the text.
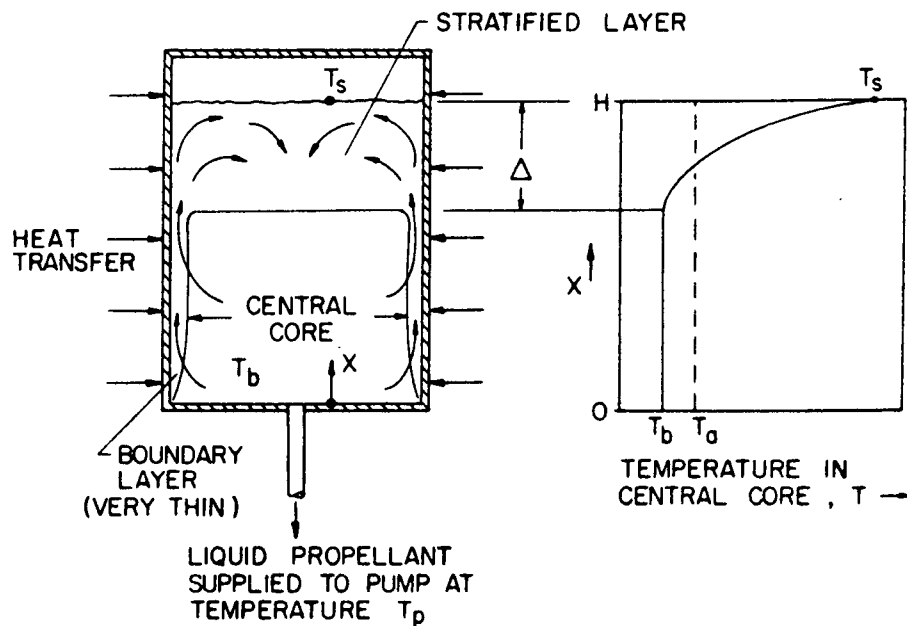
Fig. 1   Stratification in a Propellant Supply Tank
Due to Heat Transfer

decends slowly in the center. The temperature at the liquid
surface increases as the process proceeds. Since warm fluid
continues to rise along the wall, the heated fluid layer at
the top becomes thicker. This layer is referred to as the
stratified layer. The mechanism by which it is formed is
called stratification. Detailed studies of this phenomenon
are described in some of the references.[1-6]

A number of difficulties have been encountered in liquid
propellant rocket technology which have been traced directly
to the presence of stratification in supply tanks. Among
these, one of the most serious involves the potential
problem of cavitation in the supply pumps,[3,4,7-11] especial-
ly near the end of the fuel-burning period when fluid in
the stratified layer has descended to the bottom of the
tank. This liquid is hotter than that discharged earlier in
the burning period. Thus, its vapor pressure is considerably
higher so that the onset of cavitation of this liquid, when
it reaches the pumps, is far more probable.[3,4,7-9] Once
severe pump cavitation is established, the liquid flow may
be choked off so that premature combustion burnout may occur

2

in the engine due to lack of propellant supply.[4,10,11] If this should happen when a substantial portion of the liquid still remains in the supply tanks, it is conceivable that the vehicle could fail to accomplish its mission.[4,10,11] Or, on the other hand, even if mission accomplishment should result, it might be achieved at the expense of a considerable weight penalty if engine thrust is terminated due to cavitation with a large amount of unburned fuel and oxidizer still remaining in the supply tanks. A final possibility is that such cavitation can be prevented by increasing the supply pressure. This requires increased structural strength of the tank, however, so a weight penalty is incurred with this alternative also.[3,9,11,12] Nevertheless, this is the most commonly used procedure for avoiding cavitation.

Several methods of eliminating the undesirable effects of stratification have been studied, and each of these possesses some disadvantages in terms of effectiveness, cost, weight, power requirements, complexity, and unreliability. The techniques suggested previously include the use of baffles and bubble lift pumps.[8,9,12]

The present paper describes a different method for decreasing the stratification-induced propellant supply temperature rise during drainage from the supply tank. To the knowledge of the authors, this procedure has not been reported previously. Experimental data are given to provide evidence of its future potential as a practical technique. A small scaled-down tank was used to obtain these measurements. Water was incorporated as the test liquid. The most favorable measurements exhibit a rise in exit fluid temperature approximately 44% less than the corresponding rise which occurred during a conventional tank discharge process. This improvement indicates that a considerable decrease in maximum vapor pressure could be obtained for the liquid supplied to the pumps, thus enhancing the prevention of pump cavitation.

3

The proposed technique relies upon proper adjustment of the flow distribution for the liquid leaving the tank through multiple outlets. There is no requirement for additional pumps, power-driven mixers, actuation of valves during flight, or any other device containing moving mechanical parts and needing auxiliary power for its operation. Thus, the technique possesses certain inherent advantages of high reliability. It is clear, however, that careful engineering design, additional development, and increased complexity of construction would be necessary in order to produce favorable results with a full scale system. The following section contains a more detailed description of the method.

INFLUENCE OF STRATIFICATION ON PROPELLANT SUPPLY

Consider the stratification condition depicted in Fig. 1 as being representative of the situation just prior to engine ignition. The liquid can be considered to be initially at bulk temperature, T_b, but heat transfer from the container wall has increased the temperature level of a portion of the liquid which has risen to the top. Here there is a stratified layer of liquid of thickness Δ which posseses the temperature distribution indicated in Fig. 1. Once ignition has occurred the liquid level decreases with time and, simultaneously, heat transfer to the liquid continues during the transient time period when the liquid is being discharged.

If the total heat transfer occurring during the discharge period is small relative to that which has occurred prior to ignition, then the propellant supply temperature, T_p, varies with time in the same manner as T varies with height in Fig. 1. This result is illustrated by the solid line in Fig. 2. The propellant temperature first remains constant at the bulk temperature T_b for a time t_b before increasing. If all of the propellant is subsequently discharged from the tank, then the last portion of liquid leaving the container as it becomes empty (at time t_e) possesses temperature T_s, the liquid surface temperature at the initial height H above
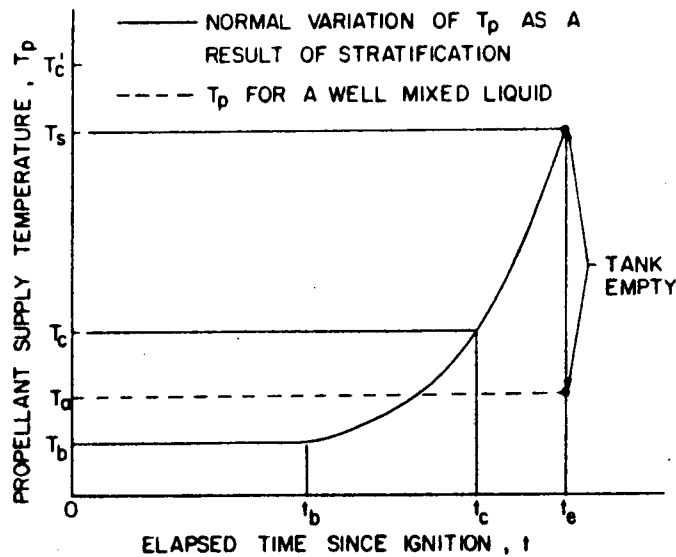
4

Fig. 2   Influence of Stratification on
Propellant Supply Temperature

the outlet, as shown in Fig. 1. If the heat transfer occurring during the burning period is appreciable, as it sometimes is when aerodynamic heating is involved, then the resulting T_p vs t curve lies somewhat above the one shown in Fig. 2 on the right hand side. However, this transient heating effect is omitted from the remaining discussion for purposes of clarity. The influence of the heat transfer during the discharge period can easily be incorporated as a later extension of the present study, since its occurrence does not disrupt nor in any way invalidate the general approach developed here.

Now consider the situation in which severe pump cavitation occurs whenever the propellant supply temperature exceeds a cavitation value, T_c. If such a condition causes termination of engine burning, then the total burning time is t_c instead of t_e as shown in Fig. 2. In this case a substantial portion of the initial propellant may be left in the tank without being consumed. This condition can be averted by increasing T_c to a higher value, T_c', by increasing the tank pressure. The higher pressure is sometimes achieved by employing a foreign gas (different from the vapor of the liquid

5

propellant) as a pressurizing agent. This usually requires
a propellant tank with increased structural strength capable
of sustaining the increased supply pressure, thus resulting
in the weight penalty mentioned previously.

A second technique involves the use of mixers or pumps which
impart motion to the liquid in the supply tank to bring
colder liquid from the lower portion of the tank into contact
with the hotter liquid at the top to produce a mixture at an
intermediate temperature level. If the liquid in the tank
were completely mixed just prior to engine ignition, then the
entire mass of liquid would be at a uniform temperature,
T_a, the average temperature for the initial stratified
temperature profile illustrated in Fig. 2. In this ideal
case the propellant supply temperature T_p is constant
throughout the burning period with $T_p = T_a$, and cavitation
does not occur as long as the supply pressure is sufficient
to make $T_c > T_a$. This desirable result is achieved only at
the expense of the increased complexity associated with the
incorporation of mixers, conventional pumps, bubble lift
pumps, or other devices which can adequately prevent the
hotter fluid from rising to the top and remaining there
permanently. Baffles, which can be used to deflect the warm
fluid rising near the tank wall toward the central core,
offer a means of inducing some mixing without requiring the
complexity of any mechanically moving parts nor relying upon
the actuation of auxiliary valves. The use of baffles
possesses several advantages over other techniques that have
been considered, but this method suffers from the fact that
the baffles are effective in preventing the stratification
buildup only during the early portion of the transient
stratification period. Further information on the techniques
mentioned in this paragraph, including the advantages and
disadvantages of each, can be obtained by referring to the
appropriate references cited in the Introduction. The
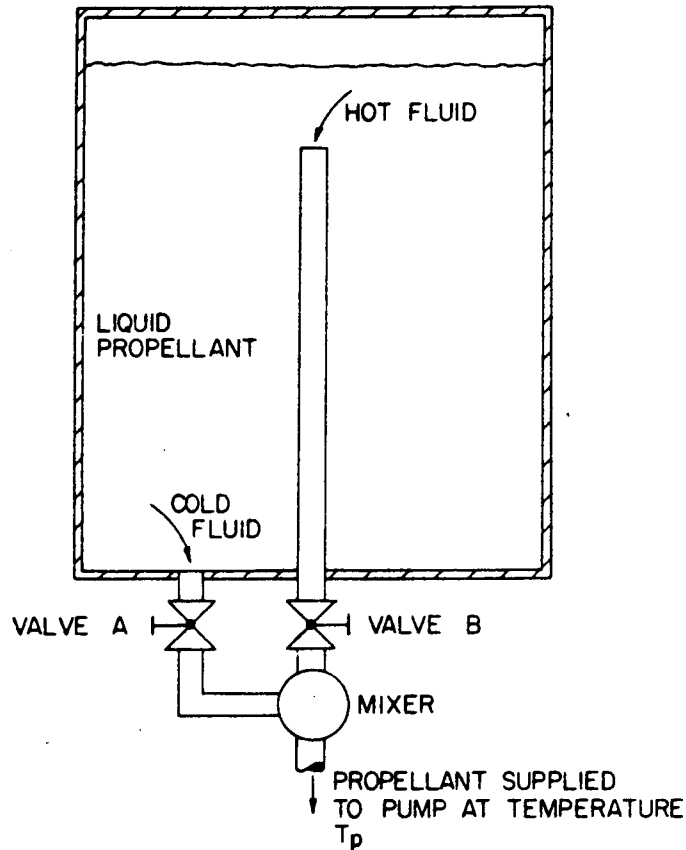following section of the paper describes an alternate method,

Fig. 3   Propellant Tank with Two Outlet Tubes

not previously reported, which forms the basis of the present study.

USE OF MULTIPLE OUTLETS

It is conventional practice to connect the propellant line or lines to the bottom of the propellant supply tank (Fig. 1). It is suggested here, however, that additional supply outlets can be used to remove the hotter fluid near the liquid surface continuously throughout the discharge process. Thus, the hottest fluid does not remain in the tank until the very end of the discharge process, nor is it necessary to employ a mixing device of some kind to reduce the undesirable influence of the stratification on the propellant supply temperature.

A schematic diagram of an initial design, incorporating only two outlets, is shown schematically in Fig. 3. With this arrangement, Valve A can be adjusted so that it constitutes

a sufficiently large flow restriction (relative to Valve B) so that an appropriate flow of hot fluid from the top is obtained. The hot and cold streams are brought together in the Mixer where an intermediate temperature is achieved for the single mixed fluid stream which flows to the pump. Two difficulties become immediately apparent at this point, and they complicate the detailed design of such a system:

1. The flow of fluid from the upper outlet causes a variation in the temperature distribution in the stratified layer in the vicinity of the liquid surface.

2. During the discharge process the upper outlet becomes completely inoperative as soon as the liquid level drops below the outlet.

The first item appears to be an inescapable feature of the process which would need to be dealt with carefully in order to arrive at a final detailed design which derives the maximum possible benefit from the method. The second item suggests that it would be desirable if the mechanism could be made to operate throughout the discharge process. This can be accomplished by use of multiple outlets (more than two) located at various heights in the tank. Then, as the liquid level drops below the uppermost outlets, causing them to become inoperative, outlets at lower locations continue to operate and become effective as the hotter liquid is lowered into their vicinity.

Although the use of several tubes having different lengths may give rise to desirable propellant supply temperature characteristics, the additional weight and the need to structurally support each of them within the supply tank appears to make this approach somewhat impractical. Therefore, in this study a compromise was sought which required only two outlet tubes, as shown in Fig. 3, but still provided for multiple outlets at various heights inside the supply tank. This was accomplished by incorporating holes of different sizes along the length of the longer tube shown in Fig. 3 so that liquid was continuously removed at all
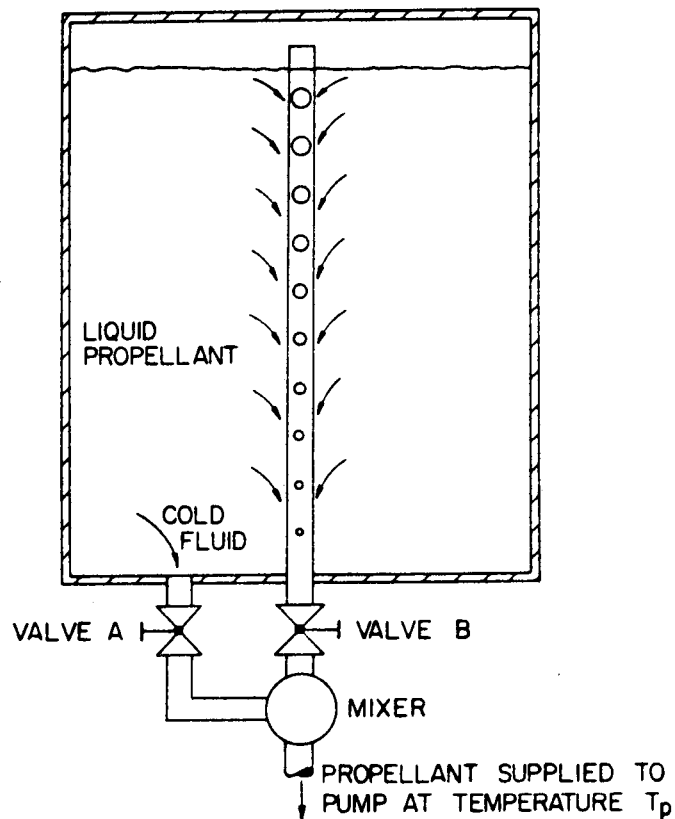
8

Fig. 4   Propellant Tank with Multiple Outlets and
Two Outlet Tubes

levels from the tank as illustrated in Fig. 4.   The design
of this kind of system involves the difficult question of
the proper sizes of the holes in the tube, the number of
holes to be used, and the distribution of the holes along
the length of the tube.   It was reasoned that the holes
located along the upper portion of the tube should be the
largest, with smaller holes further down.   This arrangement
should cause a sizeable flow of the hot fluid from the
vicinity of the liquid surface very early in the discharge
period, while producing a relatively larger restriction to
the flow from the lower portion of the tank.   Then, when
the liquid surface descends and causes the uppermost holes
to become inoperative, the holes further down become more
dominant.   Since there are holes allowing flow of the
warmer liquid near the free surface at all levels along the

tube, this liquid is continuously removed and mixed with
colder fluid from the lower portion of the tank. The fact
that the flow restriction for the fluid near the surface
increases when smaller holes are encountered as it decends
is partially compensated for by the decreasing length of the
flow path between the liquid surface and the Mixer.

The ultimate goal would be the achievement of a propellant
supply temperature which is essentially constant throughout
the discharge period (as indicated by the dashed line in
Fig. 2, for example). This may be possible with the proper
size and distribution of the various holes along the
discharge tube and, perhaps, even without the need for the
second discharge line containing Valve A (see Fig. 4). This
goal represents a problem of considerable magnitude and one
which can probably be approached by means of a detailed
analysis of the transient flow and thermal conditions in
the tank during discharge of the liquid. Such an analytical
study was not performed in the present research, however,
since this investigation represented only a preliminary
feasibility study of the technique in which complexity was
avoided wherever possible. Therefore, a small experimental
program was executed using the general arrangement shown in
Fig. 4. Several different tubes with various hole configura-
tions were used, and Valves A and B were adjusted in an
attempt to obtain a measured outlet temperature whose
maximum value during the entire discharge process was as low
as possible. These experimental results are described in
the following section.

DESCRIPTION OF EXPERIMENTS

The experimental system contained a small tank 12 inches in
diameter and 18 inches high fabricated from 1/8-inch thick
brass. Water was used as the test fluid. The tank was
filled with room temperature water to a depth of 16 inches
prior to each test. Then, two 450 watt electrical strip
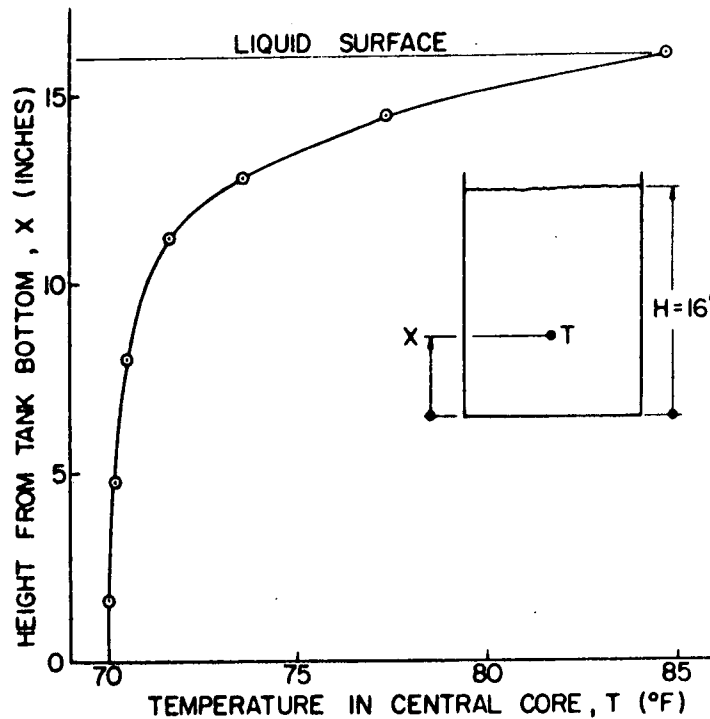heaters, firmly bolted to the outside of the tank, were

10

Fig. 5 Typical Temperature Profile as Measured in the
        Central Core just Prior to Discharge

turned on for a period of 15 minutes. The electrical power
to these heaters was then terminated, and this was followed
by a 3 minute waiting period to allow for the transient
cooling of the heaters. Then a main control valve located
below the Mixer was opened to initiate the discharge process.
Thus, gravity driven flow was used with both the liquid
surface and the outlet exposed to the atmosphere. This
caused the flow velocity to decrease somewhat during the
process. Any resulting deviation from the flow behavior
associated with actual propulsion systems was deemed to be
unimportant for purposes of this feasibility study.

Some of the energy provided by the strip heaters was lost
to the environment, some was utilized in heating up the
tank itself, and the remainder was transferred to the water.
However, as a result of the standardized 15 minute heating
period and 3 minute waiting period, the temperature distri-
bution in the liquid at the initiation of discharge was

11

essentially the same for all tests. This recurrent initial temperature distribution yielded a good basis for comparison of the various results obtained. Fig. 5 contains a typical plot of the temperature distribution in the central core, just prior to the initiation of discharge, as indicated by thermocouples located in the water at various depths beneath the surface.

The lines leading to the Mixer were 5/16-inch diameter tubing, and the Mixer itself was merely a T-connection in this small apparatus. A thermocouple located downstream from the Mixer was used to measure the equivalent propellant supply temperature, T_p, of the mixed flow. The response of this thermocouple was displayed continuously by means of a strip-chart recorder. Several different supply tubes were mounted inside the tank and tested (Figs. 3 and 4). These tubes were fabricated from 1/2-inch diameter bakelite tubing. It was felt that this kind of tubing would prevent appreciable heat transfer from the hot fluid descending in the tube, and was therefore more appropriate than metal tubing for purposes of simplicity in this feasibility study. This would not necessarily be a requirement in a perfected design for an actual propulsion system, for indeed, it may be possible to achieve better performance by allowing the hot fluid to reject much of its excess energy to the central core before it reaches the Mixer.

A sensitive pressure transducer was located at the bottom of the tank, and the signal from this transducer was also displayed on the strip-chart recorder. Since the water surface descended quite slowly during the discharge process, dynamic effects for the liquid flow in the tank were negligibly small. Thus, the variation of the pressure signal provided an instantaneous indication of the hydro-static pressure alone, which was proportional to the height of the water column in the tank. This system was calibrated so that a continuous plot of the liquid surface position as
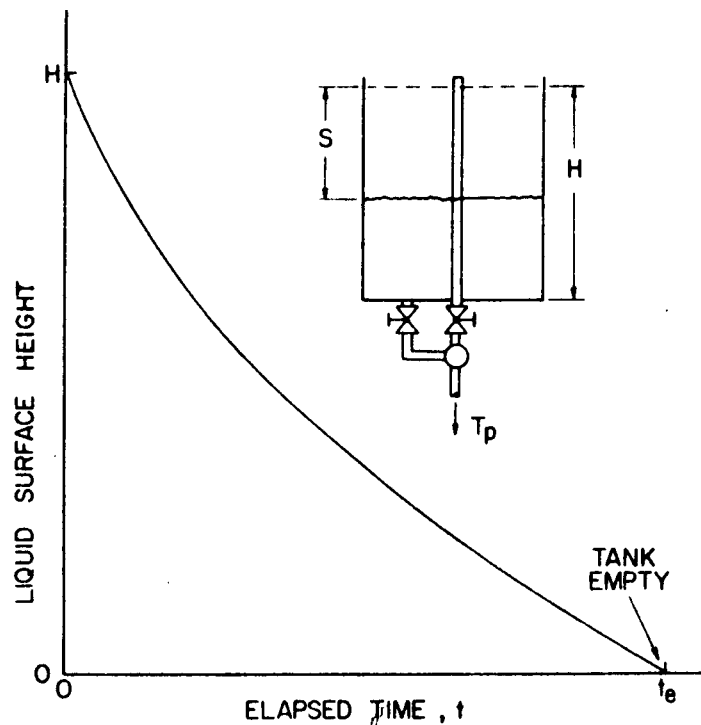
12

Fig. 6 Typical Variation of Liquid Surface Position

a function of time could be obtained during each test.

Time plots of the liquid surface height had the
general shape illustrated in Fig. 6 as a result of the
decreasing flow rate associated with gravity driven flow. If
the flow rate were constant, S would vary linearly with t
and a plot of T_p vs S would have exactly the same shape as
a plot of T_p vs t. Since S did not vary linearly with t in
these experiments (see Fig. 6), a plot of T_p vs S for a given
test was slightly different from the corresponding plot of
T_p vs t, although the two plots were qualitatively very
similar. It was found that plots of T_p vs S were somewhat
more useful than plots of T_p vs t. This was because signif-
icant variations in T_p could be easily correlated with the
corresponding instantaneous relative position of the liquid
surface with respect to the various openings in the bakelite
discharge tube inside the tank. For this reason, the two
strip chart recordings (T_p vs t and S vs t) were cross-
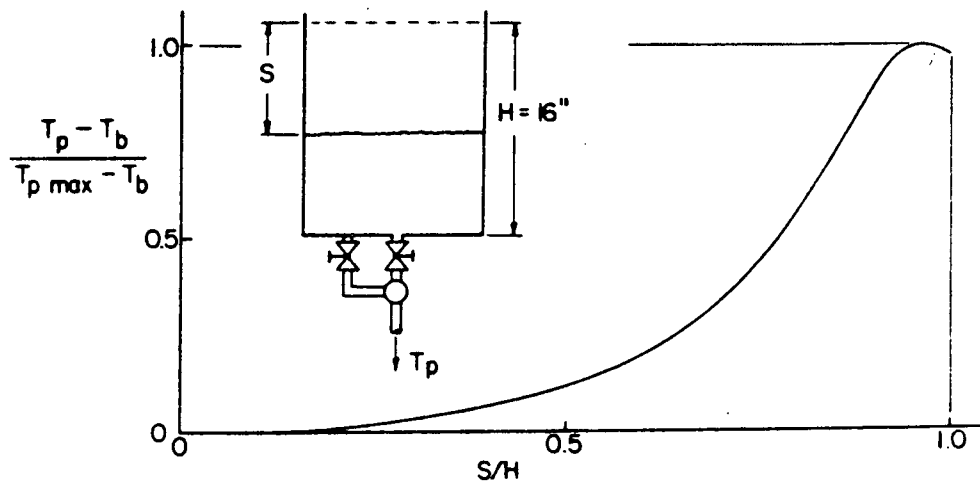plotted to yield T_p vs S.

13

Fig. 7 Measured Outlet Temperature Response for a
Conventional Discharge Process

EXPERIMENTAL RESULTS

Since the bulk water temperature, T_b, varied slightly among
the tests, comparisons between tests are facilitated by the
use of $(T_p - T_b)$, rather than T_p alone. Also, for the pur-
pose of comparing the multiple outlet tests with a correspond-
ing conventional test with drainage only from the bottom of
the tank, this temperature difference is compared with a
reference temperature difference, $(T_{p\ Max} - T_b)$, where $T_{p\ Max}$
is the maximum outlet temperature measured during the
conventional discharge process. In all cases the minimum
recorded value of T_p was essentially equal to T_b, the initial
bulk temperature of the liquid in the tank. With the two
temperature differences defined above, a convenient
dimensionless basis for comparison is achieved with plots of
$(T_p - T_b)/(T_{p\ Max} - T_b)$ as a function of S/H. Some typical
results are now presented in this manner.

Fig. 7 shows the measured outlet temperature variation for a
conventional discharge process, in the absence of an outlet
tube inside the tank, with drainage occurring only from the
bottom of the tank. As expected, the major features of the
curve are qualitatively very similar to the plot of the
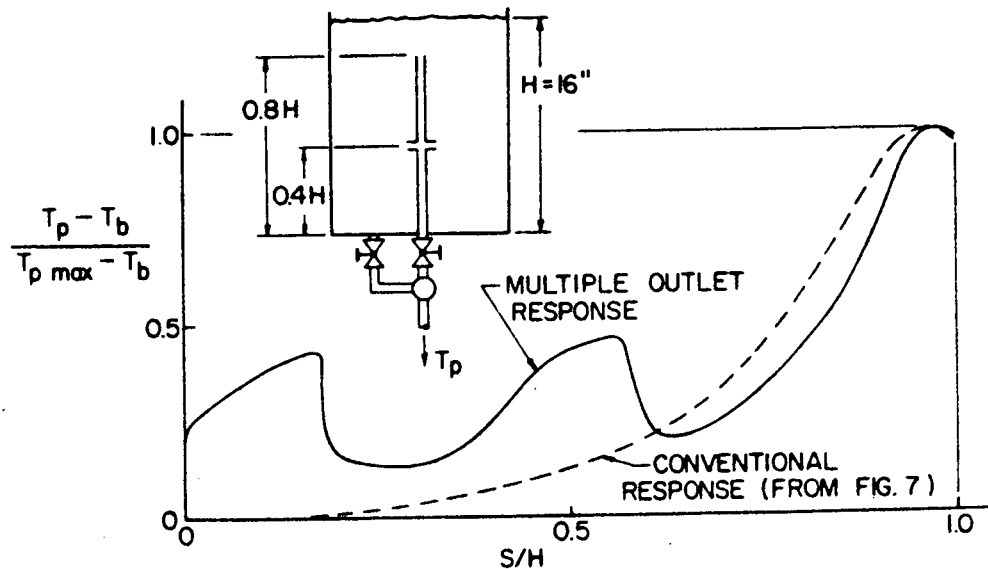initial temperature distribution, as indicated by the plot

14

Fig. 8 Comparison of Multiple Outlet Response with
Conventional Response

of T vs x in Fig. 5. There was a slight dropoff in T_p near
the end of the process. This dropoff was probably due to
heat transfer from the hot surface to the air above it during
the discharge period. The $T_{p\ Max}$-value was found to be
fairly close to the initial surface temperature, so the
dimensionless temperature response contained in Fig. 7 may
be loosely regarded as a plot of $(T_p - T_b)/(T_s - T_b)$.

Figure 8 contains a comparison of the conventional response
with a response obtained using a multiple outlet system. In
this case there were only 3 openings in the upper discharge
tube, one consisting of the open upper end of the tube
located about 3 inches below the initial surface level, and
the other two consisting of 3/16-inch diameter holes located
about 6 1/2 inches above the bottom of the tank. The
behavior indicated by the temperature response is easily
interpreted in terms of the locations of these outlet
openings. Early in the process there was considerable flow
of hot fluid through the upper opening, and this caused the
outlet temperature to rise. Then, the liquid surface
dropped below this opening causing that flow to be terminated,
and the outlet temperature rapidly dropped. When the hot
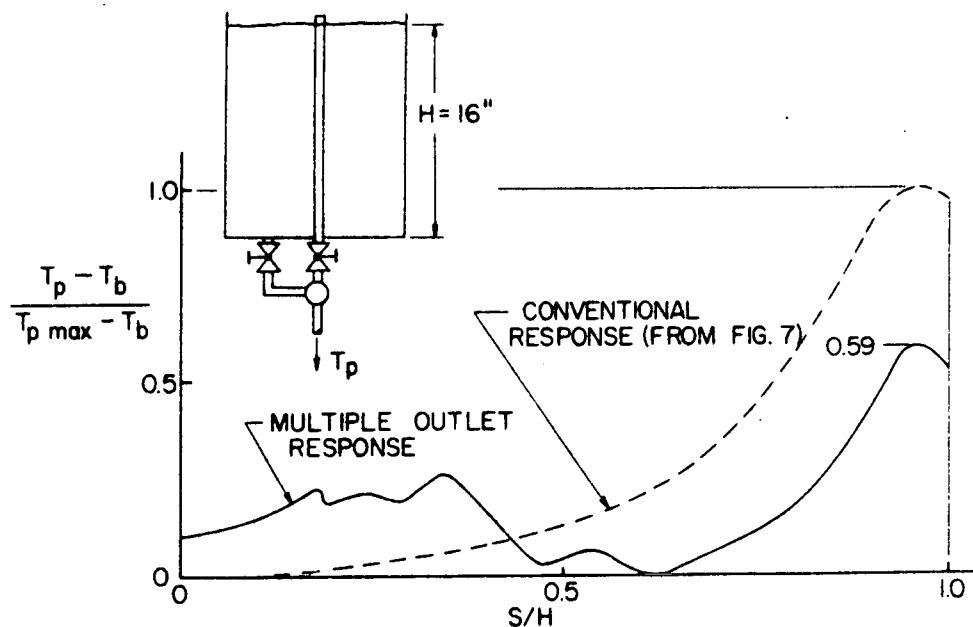fluid near the surface descended into the vicinity of the two

15

Fig. 9   Comparison of Multiple Outlet Response with
Conventional Response

lower openings the outlet temperature again rose temporarily,
and then decreased again as the surface dropped below these
openings. At the end of the process the outlet temperature
still rose to the same maximum level as in the case of the
conventional test, so evidently the flow of the hot fluid
through the upper outlet tube was not sufficient to effect
any improvement with regard to the maximum outlet temperature.
Obviously the arrangement used did not produce any major
improvement in this instance, but it will be shown that
considerable improvement can be attained with a more favor-
able distribution of the outlets.

Figures 9 and 10 illustrate typical responses for upper out-
let tubes containing many 1/8-inch diameter holes. Both
of these cases exhibit substantial improvement over the
conventional situation. Figure 9 shows a case in which the
maximum outlet temperature rise was lowered by 41% relative to
that of the conventional test. It appears from the response
curve that the sizeable rise in T_p near the end of the process
probably could have been lowered if a substantial flow of
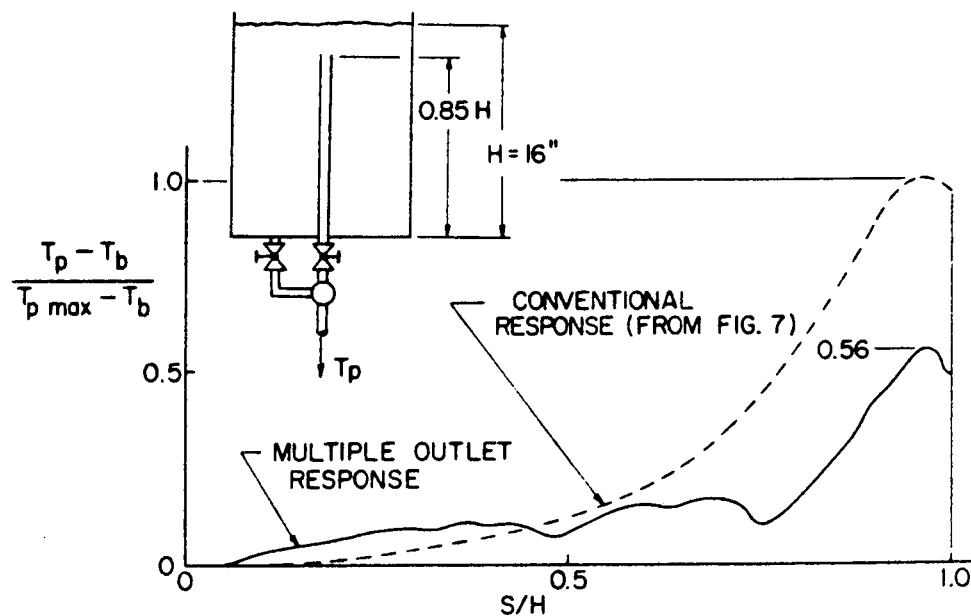hot fluid could have been sustained throughout the entire

16

Fig. 10   Comparison of Multiple Outlet Response with
Conventional Response

test.   It is clear from the low values of T_p recorded in the
middle portion of the test that very little flow of the
hotter liquid was obtained when the liquid surface was
roughly halfway to the bottom.   This can be seen by referring
to the response curve of Fig. 9 in the range of S/H between
0.45 and 0.65.

Figure 10 shows the response curve for a similar situation,
but with a somewhat more favorable arrangement of the 1/8-
inch diameter holes in the upper discharge tube.   Also, in
this case the open end of the tube was beneath the liquid
surface initially instead of being above it (see insets in
Figs. 9 and 10).   A moderate flow of hot fluid was maintained
throughout most of the process, but this did not eliminate
the substantial temperature rise near the end that has
characterized each of the responses previously discussed.
The maximum rise indicated in Fig. 10 is slightly less than
that exhibited in Fig. 9, however, which does represent a
more desirable configuration for the outlet system.   The
maximum rise was 44% below that of the conventional test.
This represents the most favorable performance achieved in

17

this study. It is evident from the response that the flow of the hotter fluid was quite small in the early portion of the process, but had a gradually increasing trend as the discharge progressed.

It should be emphasized that the arrangements of the outlet holes used for obtaining the responses in Figs. 9 and 10 were established largely by trial and error, but with the application of some intuitive reasoning that developed in analyzing previous responses as indicated by the foregoing discussion. A total of about 25 tests were conducted, although only a few typical responses are presented here. It should also be mentioned that the total discharge times were not the same for all tests due to the different valve settings and different outlet hole configurations. Actually, only two different valve settings were used, and the drainage times for all tests were in the range from 6 to 12 minutes. The tests associated with Figs. 7 and 8 required approximately 6 1/2 minutes, while those associated with Figs. 9 and 10 required about 11 minutes.

It appears that a desirable modification of the design associated with Fig. 10 should provide a greater flow of hot fluid in the early stages of the process and slightly greater flow in the intermediate stages. If such a design is achieved, it may be possible to obtain a considerable attenuation of the sharp temperature rise which occurred near the end of each of the tests conducted in this study. Indeed, it may even be possible to achieve a nearly uniform value of T_p throughout the entire process with a properly optimized design of the multiple outlet system.

CONCLUSION

It is concluded that the multiple outlet technique described in this paper is capable of effecting significant reductions in the stratification-induced propellant supply temperature rise. In this feasibility study the most favorable experimental results exhibited a 44% decrease in this

temperature rise. These preliminary measurements indicate that improved outlet designs should make it possible to obtain further reductions in the maximum outlet temperature, but the refinement of such designs will require additional development effort. The proposed technique does not require auxiliary power, nor does it necessitate the use of any moving parts. Hence, the method is potentially capable of offering high reliability. If the technical advantages associated with this approach are sufficient to warrant further study on a practical basis, then analyses accounting for weight, cost and fabrication considerations would be desirable.

ACKNOWLEDGMENT

NOTATION

H	initial height of the liquid surface above the bottom of the supply tank
S	instantaneous position of the liquid surface relative to the initial liquid surface height
t	elapsed time since initiation of discharge
t_b	time at which propellant supply temperature begins to rise
t_c	time at which onset of cavitation occurs
t_e	total time required to empty the supply tank
T	initial temperature in the central core
T_a	initial average temperature of the liquid in the supply tank
T_b	bulk temperature of the liquid in the supply tank
T_c	propellant supply temperature at onset of cavitation
T'_c	propellant supply temperature at onset of cavitation

	under increased pressure
T_P	propellant supply temperature
$T_{P\ Max}$	maximum value of the propellant supply temperature
T_s	initial temperature at the liquid surface
x	distance from the bottom of the supply tank
Δ	initial thickness of the stratified layer

REFERENCES

1. D. M. Tellep and E. Y. Harper, "Approximate Analysis of Propellant Stratification", AIAA Journal, Vol. 1, No. 8, Aug. 1963, pp. 1954-1956

2. R. G. Schwind and G. C. Vliet, "Observations and Interpretations of Natural Convection and Stratification in Vessels", Proceedings of the 1964 Heat Transfer and Fluid Mechanics Institute, edited by W. H. Giedt and S. Levy, Stanford University Press, 1964, pp. 51-68

3. T. E. Bailey and R. F. Fearn, "Analytical and Experimental Determination of Liquid-Hydrogen Temperature Stratification", Advances in Cryogenic Engineering, Vol. 9, edited by K. D. Timmerhaus, 1964, pp. 254-264

4. J. W. Tatom, W. H. Brown, L. H. Knight, and E. F. Coxe, "Analysis of Thermal Stratification of Liquid Hydrogen in Rocket Propellant Tanks", Advances in Cryogenic Engineering, Vol. 9, edited by K. D. Timmerhaus, 1964, pp. 265-272

5. R. W. Arnett and D. R. Millhiser, "A Theoretical Model for Predicting Thermal Stratification and Self Pressurization of a Fluid Container", Proceedings of the Conference on Propellant Tank Pressurization and Stratification, Vol. II, George C. Marshall Space Flight Center, NASA, Huntsville, Alabama, Jan. 20-21, 1965, pp. 1-20

6. J. A. Clark and H. Z. Baraket, "Transient, Laminar Free-Convection Heat and Mass Transfer in Closed, Partially Filled, Liquid Containers", Proceedings of

the Conference on Propellant Tank Pressurization and Stratification, Vol. II, George C. Marshall Space Flight Center, NASA, Huntsville, Alabama, Jan. 20-21, 1965, pp. 119-189

7. B. D. Neff and C. W. Chiang, "Free Convection in a Container of Cryogenic Fluid", Advances in Cryogenic Engineering, Vol. 12, edited by K. D. Timmerhaus, 1966, pp. 112-124

8. B. D. Neff, "Investigation of Stratification Reduction Techniques", Proceedings of the Conference on Propellant Tank Pressurization and Stratification, Vol. II, George C. Marshall Space Flight Center, NASA, Huntsville, Alabama, Jan. 20-21, 1965, pp. 21-42

9. D. C. Pedreyra, "Stratification Reduction by Means of Bubble Pumps", Proceedings of the Conference on Propellant Tank Pressurization and Stratification, Vol. II, George C. Marshall Space Flight Center, NASA, Huntsville, Alabama, Jan 20-21, 1965, pp. 43-60

10. H. M. Campbell, Jr., Fluid Quality in a Self-Pressurized Container Discharge Line, NASA TM X-53330, George C. Marshall Space Flight Center, Huntsville, Alabama, Aug. 18, 1965

11. I. I. Pinkel et al., Pump Technology, NASA SP-5053, Conference on Selected Technology for the Petroleum Industry, Part VI, Lewis Research Center, NASA, Cleveland, Ohio, Dec. 8-9, 1965, pp. 81-101

12. G. C. Vliet and J. J. Brogan, "Experimental Investigation of the Effect of Baffles on Natural Convection Flow and on Stratification", Proceedings of the Conference on Propellant Tank Pressurization and Stratification, Vol. II, George C. Marshall Space Flight Center, NASA, Huntsville, Alabama, Jan. 20-21, 1965, pp. 61-86